MODELLISTICA E CALCOLO SCIENTIFICO

MODELING AND SCIENTIFIC COMPUTING

MOX-Report No. 57/2023

An optimally convergent Fictitious Domain method for interface problems

Regazzoni, F.

MOX, Dipartimento di Matematica
Politecnico di Milano, Via Bonardi 9 - 20133 Milano (Italy)

mox-dmat@polimi.it https://mox.polimi.it

An optimally convergent Fictitious Domain method for interface problems

Francesco Regazzoni[1,*]

[1] MOX - Dipartimento di Matematica, Politecnico di Milano, Milan, Italy
[*] *Corresponding author* (`francesco.regazzoni@polimi.it`)

Abstract

We introduce a novel Fictitious Domain (FD) unfitted method for interface problems that achieves optimal convergence without the need for adaptive mesh refinements nor enrichments of the Finite Element spaces. The key aspect of the proposed method is that it extends the solution into the fictitious domain in a way that ensures high global regularity. Continuity of the solution across the interface is enforced through a boundary Lagrange multiplier. The subdomains coupling, however, is not achieved by means of the duality pairing with the Lagrange multiplier, but through an L^2 product with the H^1 Riesz representative of the latter, thus avoiding gradient jumps across the interface. Thanks to the enhanced regularity, the proposed method attains an increase, with respect to standard FD methods, of up to one order of convergence in energy norm. The Finite Element formulation of the method is presented, followed by its analysis. Numerical tests demonstrate its effectiveness.

Keywords: Interface problems, Fictitious Domain method, Unfitted methods, Generalized saddle-point problems, Optimal convergence rate.

1 Introduction

Interface problems, which occur in various application fields, involve the interaction between two subdomains that share a common interface. These subdomains are characterized by differential problems featuring distinct operators and/or coefficients, coupled through suitable conditions at the interface, which typically express conservation principles (e.g., conservation of mass and momentum). Illustrative instances of interface problems include heat transfer problems with discontinuous coefficients and fluid-structure interaction problems.

The numerical approximation of such problems is often based on meshes that are fitted to the interface [4, 16, 25, 50]. In many cases, however, the fitted approach is not suitable or appropriate, and unfitted approaches in which the interface is allowed to cross mesh elements are preferable, e.g. when the domains have a complicated shape or when the interface is moving. As a motivating example we consider fluid-structure interaction problems, in which the motion of the solid domain would necessitate, if fitted methods were used, continuous (and time-consuming) remeshing, or the deformation of a preconstructed mesh, as in Arbitrary Eulerian-Lagrangian (ALE) methods [7, 17, 34], which however places severe limitations on the range of displacements that can be treated. Because of the low regularity of the solution across the interface, however, the Finite Element method (FEM) applied to meshes that are not fitted at the interface leads to suboptimal convergence rates [4], unless ad hoc expedients are introduced into the method [37], such as modifying or enriching the basis functions with special elements that satisfy the interface conditions [38–40, 51] or discontinuous elements possibly in combination with Nitsche's method [1, 23, 33], in the spirit of CutFEM (cut Finite Element Method) [18, 19] or XFEM (extended Finite Element Method) [42].

An attractive approach to interface problems, which falls into the family of unfitted methods, is the Fictitious Domain (FD) method, which consists of extending the solution defined on one subdomain to the other subdomain, the latter being often enclosed into the former, and on defining a new differential problem whose solution, if restricted to the external subdomain, coincides with the one of the original problem. FD domain methods (also known as domain embedding methods) were introduced to deal with differential problems defined in complex geometries, by embedding the computational domain in geometries of simpler shape [30, 35, 45]. Moving from the Immersed Boundary Method for fluid-structure interaction problems [44], the FD method has been applied to the treatment of interface problems [11, 14]. Typically, the solution defined in the external subdomain is extended so that it coincides with the solution defined in the internal subdomain, a constraint that is imposed by distributed Lagrange multiplier (DLM), leading to the so–called DLM/FD method [3, 12, 13, 31, 48, 49]. Such method is particularly suitable in the context of fluid-structure problems, whereby the fluid can be solved on a fixed Eulerian mesh, without the need of following the movement of the structure, which is solved on an independent Lagrangian mesh. However, the DLM/FD method gives no guarantee that the solution of the extended problem is smooth; indeed, because of the way such an extension is constructed, the solution typically features discontinuities in the normal derivatives across the interface, thus limiting the order of convergence [3, 4]. To overcome this issue, in the context of domain embedding, in [9] an adaptive solution method is proposed that relies on a nested inexact preconditioned Uzawa iteration. A current trend to alleviate accuracy problems of the DLM/FD method relies on cutFEM or XFEM, namely on enriching or duplicating degrees of freedom at the interface [27, 46, 47]. Compared with standard FD methods, however, these methods come at the price of some computational challenges, related e.g., to the need of tracking the interface position and its intersections with mesh elements [1, 26, 41], as well as a certain implementation effort or intrusive changes in existing software packages [1]. An alternative to the DLM/FD method is to extend the solution by imposing only the continuity at the interface, through a boundary Lagrange multiplier (BLM) [2, 5, 15]. However, the Lagrange multiplier induces a jump in the conormal derivative of the solution across the interface, thus making the BLM/FD method suffer from similar convergence issues to the DLM/FD method [2].

The aim of this work is to propose an unfitted FD method for interface problem, that is able to achieve, in case of regular data, optimal convergence order, without resorting, as for existing approaches, to adaptive mesh refinements or modifications and/or enrichments of the FEM space, with their consequent computational and implementation challenges. The idea behind the proposed method is to extend the solution into the fictitious domain in a way that yields high global regularity. Unlike the DLM/FD method, the extension of the external domain solution is not forced to coincide with the internal domain solution, but only continuity at the interface is imposed through a BLM. However, unlike the BLM/FD method, we do not impose consistency with respect to the original problem directly through the duality pairing with the Lagrange multiplier, but rather through the L^2 product with an additional distributed field. Such field is in fact the H^1 Riesz representative of the Lagrange multiplier composed with the trace operator, and is obtained by introducing an additional equation in the internal domain, namely a Poisson problem with reaction. Remarkably, the proposed method can be easily implemented in standard FEM software packages.

The outline of this paper is as follows. In Section 2, we introduce the class of interface problems that are addressed in this work. In Section 3, we present existing FD formulations to approximate the problems introduced above. Then, in Section 4, we introduce our proposed FD formulation. In Section 5, we introduce its Finite Element formulation and we carry out its analysis. Finally, in Section 6, we present some numerical tests.

Concerning the notation, in this work we denote by $\|\cdot\|_{s,\Omega}$ the usual norm in the Sobolev space $H^s(\Omega)$. In particular, $\|\cdot\|_{0,\Omega}$ denotes the $L^2(\Omega)$ norm. Similarly, we denote by $(\cdot,\cdot)_{s,\Omega}$ the inner product in the Sobolev space $H^s(\Omega)$. We denote the lines of grouped equations by subscript roman cardinal numbers. For example, the lines of equation (1) are referred to as $(1)_{\mathrm{I}}$, $(1)_{\mathrm{II}}$, and so on.

2 Interface problems

Let $\Omega \in \mathbb{R}^d$ (for $d = 2, 3$) be a bounded domain, partitioned into two non-overlapping subdomains Ω_1 and Ω_2 (i.e. $\overline{\Omega} = \overline{\Omega}_1 \cup \overline{\Omega}_1$ and $\Omega_1 \cap \Omega_2 = \emptyset$). In this paper we will assume for simplicity that one of the two subdomains (namely Ω_2) does not touch the boundary of Ω (see Fig. 1), although the results are easily generalized without this assumption. Then, we will refer to Ω_1 and to Ω_2 as the external and internal subdomains respectively, and we will denote by $\Gamma = \partial\Omega_2$ the interface between the two subdomains. We assume that both $\partial\Omega$ and Γ are sufficiently regular (for simplicity, let us consider $\mathcal{C}^\infty$ regularity). We denote by $\mathbf{n}_i$, for $i = 1, 2$, the unit vector, normal to the boundary and pointing outward from Ω_i. Finally, let us consider a partition of the external boundary $\partial\Omega$ into the non-overlapping (possibly empty) subsets Γ_{D} and

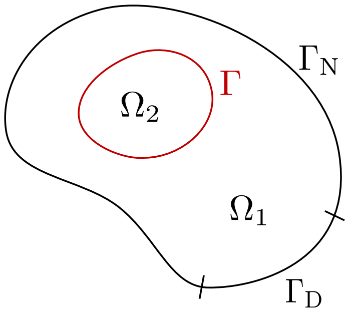

Figure 1: Computational domain Ω partitioned into the subdomains Ω_1 and Ω_2. The red curve represents the interface Γ. The boundary of Ω is split into Γ_D and Γ_N.

Γ_N.

We consider the following general form of interface problem:

$$\begin{cases} \mathcal{L}_1 \tilde{u}_1 = f_1 & \text{in } \Omega_1, \\ \mathcal{L}_2 \tilde{u}_2 = f_2 & \text{in } \Omega_2, \\ \tilde{u}_1 = \tilde{u}_2 & \text{on } \Gamma, \\ \partial^{\mathcal{L}_1}_{\mathbf{n}_1} \tilde{u}_1 + \partial^{\mathcal{L}_2}_{\mathbf{n}_2} \tilde{u}_2 = 0 & \text{on } \Gamma, \\ \tilde{u}_1 = 0 & \text{on } \Gamma_\mathrm{D}, \\ \partial^{\mathcal{L}_1}_{\mathbf{n}_1} \tilde{u}_1 = 0 & \text{on } \Gamma_\mathrm{N}, \end{cases} \tag{1}$$

where $\mathcal{L}_i$ are second order differential operators (for $i = 1, 2$), and $\partial^{\mathcal{L}_i}_{\mathbf{n}}$ are their conormal derivatives in direction $\mathbf{n}$, while $f_i \in L^2(\Omega_i)$ denote forcing terms. We consider homogeneous Dirichlet and Neumann boundary conditions on the subsets Γ_D and Γ_N, respectively.

A paradigmatic example is when both $\mathcal{L}_i$ are associated with the Laplace operator, albeit with different coefficients ($\mu_1 \neq \mu_2$) in the two subdomains:

$$\begin{aligned} \mathcal{L}_i u &= -\mu_i \Delta u, \\ \partial^{\mathcal{L}_i}_{\mathbf{n}} u &= \mu_i \nabla u \cdot \mathbf{n}. \end{aligned} \tag{2}$$

In this case, the operator $\mathcal{L}_i$ is associated with the following bilinear form, defined on the set $V \subseteq \Omega$:

$$a_i^V(u, w) = \int_V \mu_i \nabla u \cdot \nabla w.$$

Generally speaking, we denote by a_i^V, for $i = 1, 2$ the bilinear forms associated with the operators $\mathcal{L}_i$, such that $a_i^\Omega = a_i^{\Omega_1} + a_i^{\Omega_2}$ and for which the Green formula holds (with $E \in \{\Omega, \Omega_1, \Omega_2\}$):

$$\int_E (\mathcal{L}_i u)\, v = a_i^E(u, v) - \langle \partial^{\mathcal{L}_i}_{\mathbf{n}} u, v \rangle_{\partial E}.$$

With the symbol $\langle \cdot, \cdot \rangle_{\partial E}$ we denote the duality pairing between $H^{1/2}(\partial E)$ and its dual $H^{-1/2}(\partial E)$, where the trace operator applied to the second argument is left implicit. Then, it is well-known that the weak formulation of (1) reads as follows.

Problem 1. *Find* $\tilde{u} \in H^1_{0,\Gamma_\mathrm{D}}(\Omega) = \{\tilde{v} \in H^1(\Omega), \tilde{v}\big|_{\Gamma_\mathrm{D}} = 0\}$ *such that*

$$a_1^{\Omega_1}(\tilde{u}, \tilde{v}) + a_2^{\Omega_2}(\tilde{u}, \tilde{v}) = \int_{\Omega_1} f_1 \tilde{v} + \int_{\Omega_2} f_2 \tilde{v} \qquad \forall\, \tilde{v} \in H^1_{0,\Gamma_\mathrm{D}}(\Omega). \tag{3}$$

Then, set $\tilde{u}_i = \tilde{u}\big|_{\Omega_i}$, *for* $i = 1, 2$.

3 Fictitious Domain formulations

The FD formulation of the interface problem (1) envisages two unknowns, namely u_1, an extension of $\tilde{u}_1$ to the whole Ω, and u_2, which coincides with $\tilde{u}_2$. We introduce thus the spaces $V^1 = H^1_{0,\Gamma_D}(\Omega)$ and $V^2 = H^1(\Omega_2)$, for the unknowns u_1 and u_2, respectively. Moreover, we conveniently extend the forcing term f_1 to the whole Ω (with a little abuse of notation, we keep the name f_1). Notice that also the trivial zero extension is possible.

3.1 DLM/FD formulation

We consider the following DLM/FD formulation, in which the extension is obtained by imposing, through the distributed Lagrange multiplier p, the constraint $u_1 = u_2$ on Ω_2 [3, 13, 48]. With $(H^1(\Omega_2))^*$ we denote the dual space of $H^1(\Omega_2)$, and by $\langle \cdot, \cdot \rangle_{\Omega_2}$ the duality pairing between the two spaces.

Problem 2. *Find $u_1 \in V^1$, $u_2 \in V^2$, $p \in (H^1(\Omega_2))^*$ such that*

$$\begin{cases} a_1^{\Omega}(u_1, v_1) + \langle p, v_1 \rangle_{\Omega_2} = \displaystyle\int_{\Omega} f_1 v_1 & \forall\, v_1 \in V^1, \\ a_2^{\Omega_2}(u_2, v_2) - a_1^{\Omega_2}(u_2, v_2) - \langle p, v_2 \rangle_{\Omega_2} = \displaystyle\int_{\Omega_2} (f_2 - f_1) v_2 & \forall\, v_2 \in V^2, \\ \langle q, u_1 - u_2 \rangle_{\Omega_2} = 0 & \forall\, q \in (H^1(\Omega_2))^*. \end{cases} \tag{4}$$

The well-posedness of Problem 2, as well as the equivalence to Problem 1, are studied e.g. in [3, 13]. The equivalence shall be intended through the identification $\tilde{u}_1 = u_1\big|_{\Omega_1}$ and $\tilde{u}_2 = u_2$.

To state the Finite Element approximation of Problem 2, we introduce a family $\mathcal{T}_h^1$ of regular meshes in Ω and a family $\mathcal{T}_h^2$ of regular meshes in Ω_2, and the Finite Element spaces $V_h^1 \subset V^1$, $V_h^2 \subset V^2$ and $\Lambda_h \subset (H^1(\Omega_2))^*$.

Problem 3. *Find $u_{h1} \in V_h^1$, $u_{h2} \in V_h^2$, $p_h \in \Lambda_h$ such that*

$$\begin{cases} a_1^{\Omega}(u_{h1}, w_{h1}) + \langle p_h, w_{h1} \rangle_{\Omega_2} = \displaystyle\int_{\Omega} f_1 w_{h1} & \forall\, w_{h1} \in V_h^1, \\ a_2^{\Omega_2}(u_{h2}, w_{h2}) - a_1^{\Omega_2}(u_{h1}, w_{h2}) - \langle p_h, w_{h2} \rangle_{\Omega_2} = \displaystyle\int_{\Omega_2} (f_2 - f_1) w_{h2} & \forall\, w_{h2} \in V_h^2, \\ \langle q_h, u_{h1} - u_{h2} \rangle_{\Omega_2} = 0 & \forall\, q_h \in \Lambda_h. \end{cases} \tag{5}$$

Optimal convergence estimates for Problem 3 have been proved (see [3] for Laplace equation and [13] for FSI problems), in the following form, where $C > 0$ is a suitable constant:

$$\begin{aligned} &\|u_1 - u_{h1}\|_{1,\Omega} + \|u_2 - u_{h2}\|_{1,\Omega_2} \\ &\quad \le C \left[\inf_{v_{h1} \in V_h^1} \|u_1 - v_{h1}\|_{1,\Omega} + \inf_{v_{h2} \in V_h^2} \|u_2 - v_{h2}\|_{1,\Omega_2} + \inf_{q_h \in \Lambda_h} \|p - q_h\|_{(H^1(\Omega_2))^*} \right]. \end{aligned} \tag{6}$$

The best-approximation errors at the right-hand side are typically constrained by the regularity of the solution. In particular, for piecewise polynomials of order r we have, for $s \ge 1$:

$$\inf_{v_{h1} \in V_h^1} \|u_1 - v_{h1}\|_{1,\Omega} \le h^{\min(r, s-1)} |u_1|_{s,\Omega}.$$

However, because of the way the extension of $\tilde{u}_1$ is constructed, the solution u_1 of Problem 2 coincides with the solution $\tilde{u}$ of Problem 1, which features low regularity. For example, in the case of the Laplace equation (see (2)) with $\mu_1 \neq \mu_2$, we have $u_1 \in H^s(\Omega_1)$ for some $s \in (1, 3/2)$ [4, 21, 36]. Hence, we can achieve at most convergence of order 1/2 in (6), regardless the polynomial order.

Remark 1. We notice that, thanks to the constraint $(4)_{\mathrm{III}}$, the term $a_2^{\Omega_2}(u_2, v_2)$ in $(4)_{\mathrm{II}}$ can be replaced by $a_2^{\Omega_2}(u_1, v_2)$ (see e.g. [49]). These two formulations are clearly equivalent at the continuous level, but not at the discrete one, and they can yield different results, as we show in Section 6.

3.2 BLM/FD formulation

Having established that extending $\tilde{u}_1$ so that it coincides with $\tilde{u}_2$ in Ω_2 places limitations on the global regularity of u_1, and thus on the order of convergence of the Finite Element approximation, it is natural to consider alternative extensions of $\tilde{u}_1$. One possibility is to employ a BLM rather than a DLM [2, 5, 6, 15]. Hence, we introduce the space $Q = H^{-1/2}(\Gamma)$, namely the dual of $H^{1/2}(\Gamma)$. We consider the following BLM/FD formulation.

Problem 4. *Find $u_1 \in V^1$, $u_2 \in V^2$, $\lambda \in Q$ such that*

$$\begin{cases} a_1^{\Omega}(u_1, v_1) + \langle \lambda, v_1 \rangle_\Gamma = \displaystyle\int_\Omega f_1 v_1 & \forall\, v_1 \in V^1, \\ a_2^{\Omega_2}(u_2, v_2) - a_1^{\Omega_2}(u_1, v_2) - \langle \lambda, v_2 \rangle_\Gamma = \displaystyle\int_{\Omega_2} (f_2 - f_1) v_2 & \forall\, v_2 \in V^2, \\ \langle \mu, u_1 - u_2 \rangle_\Gamma = 0 & \forall\, \mu \in Q. \end{cases} \tag{7}$$

The equivalence to Problem 1 can be proved similarly as for the DLM/FD formulation [2]. However, also the solution u_1 of Problem 4 has low global regularity. Indeed, by applying the Green formula, we get:

$$\begin{aligned} a_1^{\Omega}(u_1, v_1) &= a_1^{\Omega_1}(u_1, v_1) + a_1^{\Omega_2}(u_1, v_1) \\ &= \int_{\Omega_1} (\mathcal{L}_1 u_1)\, v_1 + \int_{\Omega_2} (\mathcal{L}_1 u_1)\, v_1 + \langle \partial_{\mathbf{n}_1}^{\mathcal{L}_1} u_1\big|_{\Omega_1}, v_1 \rangle_\Gamma + \langle \partial_{\mathbf{n}_2}^{\mathcal{L}_1} u_1\big|_{\Omega_2}, v_1 \rangle_\Gamma + \langle \partial_{\mathbf{n}_1}^{\mathcal{L}_1} u_1, v_1 \rangle_{\partial\Gamma_{\mathrm{N}}}. \end{aligned} \tag{8}$$

Hence, by $(7)_{\mathrm{I}}$, it follows that the Lagrange multiplier plays the role of jump of conormal derivative across Γ:

$$\partial_{\mathbf{n}_1}^{\mathcal{L}_1} u_1\big|_{\Omega_1} + \partial_{\mathbf{n}_2}^{\mathcal{L}_1} u_1\big|_{\Omega_2} = -\lambda.$$

Therefore, similarly as for the DLM/FD formulation, u_1 is not regular unless $\lambda \equiv 0$, which is of course a very special, and mostly uninteresting, case.

4 Augmented formulation (A-BLM/FD)

To improve the convergence rate of the FD Finite Element formulation, we design a smooth extension of $\tilde{u}_1$ inside Ω_2, in particular by requiring that $u_1 \in H^2(\Omega)$. Clearly, this goal makes sense only if the original problem (1) has a regular solution inside the subdomains Ω_i, otherwise the order of convergence would be low even for fitted methods that approximate Problem 1. This is the rationale for our assumption that $\partial\Omega$ and Γ are regular, and for the same reason we shall always assume that the forcing terms f_i are also regular.

4.1 A-BLM/FD formulation for the model problem

Let us first consider for simplicity the case $\mathcal{L}_i u = -\mu_i \Delta u$ and $\Gamma_{\mathrm{D}} = \partial\Omega$. We consider a trivial extension for f_1, namely $f_1 \equiv 0$ on Ω_2). In order to achieve global H^2 regularity, the following matching conditions should be satisfied on the interface Γ:

$$\begin{aligned} [\![u_1]\!] &= u_1\big|_{\Omega_1} - u_1\big|_{\Omega_2} = 0, \\ [\![\nabla u_1]\!] &= \nabla u_1\big|_{\Omega_1} \cdot \mathbf{n}_1 + \nabla u_1\big|_{\Omega_2} \cdot \mathbf{n}_2 = 0. \end{aligned} \tag{9}$$

These conditions not only are necessary to have $u_1 \in H^2(\Omega_2)$, but are also sufficient, knowing that $u_1 \in H^1_{0,\Gamma_{\mathrm{D}}}(\Omega_1) \cap H^2(\Omega_1) \cap H^2(\Omega_2)$. Indeed, let us take a test function $\phi \in \mathcal{D}(\Omega)$. By definition of distributional derivative and by the Green formula, from (9) it follows

$$
\begin{aligned}
{}_{\mathcal{D}'(\Omega)}\langle \Delta u_1, \phi\rangle_{\mathcal{D}(\Omega)} &= \int_\Omega u_1\,\Delta\phi = \int_{\Omega_1} u_1\,\Delta\phi + \int_{\Omega_2} u_1\,\Delta\phi \\
&= -\int_{\Omega_1} \nabla u_1\cdot\nabla\phi - \int_{\Omega_2} \nabla u_1\cdot\nabla\phi + \int_\Gamma \nabla\phi\cdot\mathbf{n}_1 [\![u_1]\!] \\
&= \int_{\Omega_1} \Delta u_1\,\phi + \int_{\Omega_2} \Delta u_1\,\phi - \langle [\![\nabla u_1]\!], \phi\rangle_\Gamma + \int_\Gamma \nabla\phi\cdot\mathbf{n}_1 [\![u_1]\!] \\
&= \int_{\Omega_1} \Delta u_1\,\phi + \int_{\Omega_2} \Delta u_1\,\phi.
\end{aligned}
$$

Since $\Delta u_1\big|_{\Omega_i} \in L^2(\Omega_i)$ for $i = 1, 2$, we have $\Delta u_1 \in L^2(\Omega)$. Moreover, as the application $u \mapsto \|\Delta u\|_{0,\Omega}$ is a norm in $H^2(\Omega) \cap H^1_{0,\Gamma_\mathrm{D}}(\Omega)$, it follows that $u_1 \in H^2(\Omega)$ [24].

A differential problem defining the extension of $\tilde{u}_1$ must therefore be at least of the fourth order, as we need to impose the two independent conditions (9) on the interface Γ. Thus, we consider the following bi-harmonic problem that defines the extension $\hat{u}_1 \in H^2(\Omega_2)$ of $\tilde{u}_1$ to the domain Ω_2:

$$
\begin{cases}
\mu_1\Delta^2\hat{u}_1 - \mu_1\Delta\hat{u}_1 = 0 & \text{in } \Omega_2,\\
\hat{u}_1 = \tilde{u}_1\big|_{\Omega_1} & \text{on } \Gamma,\\
\nabla\hat{u}_1\cdot\mathbf{n}_2 = \nabla\tilde{u}_1\big|_{\Omega_1}\cdot\mathbf{n}_2 & \text{on } \Gamma.
\end{cases}
$$

As it is better suited to a Finite Element formulation, we rewrite the bi-harmonic problem in mixed formulation, by introducing an additional variable z:

$$
\begin{cases}
-\mu_1\Delta\hat{u}_1 + z = 0 & \text{in } \Omega_2,\\
-\Delta z + z = 0 & \text{in } \Omega_2.
\end{cases} \tag{10}
$$

This leads to the following problem, namely a BLM/FD formulation augmented by the distributed field z, henceforth called augmented BLM/FD formulation (A-BLM/FD):

Problem 5. *Find $u_1 \in V^1$, $u_2 \in V^2$, $z \in V^2$, $\lambda \in Q$ such that*

$$
\begin{cases}
\displaystyle\int_\Omega \mu_1\nabla u_1\cdot\nabla v_1 + \int_{\Omega_2} z\,v_1 = \int_{\Omega_1} f_1 v_1 & \forall\, v_1 \in V^1,\\
\displaystyle\int_{\Omega_2} (\mu_2\nabla u_2 - \mu_1\nabla u_1)\cdot\nabla v_2 - \int_{\Omega_2} z\,v_2 = \int_{\Omega_2} f_2 v_2 & \forall\, v_2 \in V^2,\\
\displaystyle\int_{\Omega_2} \nabla z\cdot\nabla s + \int_{\Omega_2} zs = \langle\lambda, s\rangle_\Gamma & \forall\, s \in V^2,\\
\langle\mu, u_1 - u_2\rangle_\Gamma = 0 & \forall\, \mu \in Q.
\end{cases} \tag{11}
$$

4.2 Well-posedness, equivalence and regularity

We now study the well-posedness of Problem 5, its equivalence to Problem 1, and the regularity of its solution.

Theorem 1. *Assume $f_i \in H^{k+1}(\Omega_i)$ for $i = 1, 2$ and for some $k \geq 0$. Then, Problem 5 admits a solution (u_1, u_2, z, λ), unique in terms of $u_1\big|_{\Omega_1}$ and u_2 (that is to say, any other solution $(u_1', u_2', z', \lambda')$ satisfies $u_i' = u_i$ on Ω_i, for $i = 1, 2$). Moreover, $u_1 \in H^2(\Omega)$, $u_2 \in H^{k+3}(\Omega_2)$, $z \in H^{k+1}(\Omega_2)$ and $\lambda \in H^{k-\frac{1}{2}}(\Gamma)$. Furthermore, Problem 1 and Problem 5 are equivalent, with the identification $\tilde{u}\big|_{\Omega_1} = u_1\big|_{\Omega_1}$ and $\tilde{u}\big|_{\Omega_2} = u_2$.*

Proof. Let $u_1 \in V^1$, $u_2 \in V^2$ be a solution of Problem 5. Thanks to $(11)_{\mathrm{IV}}$, the traces of u_1 and u_2 on Γ coincide. Therefore, the function $\tilde{u} = u_1\mathbb{1}_{\Omega_1} + u_2\mathbb{1}_{\Omega_2}$ belongs to $H^1(\Omega)$. By taking test functions such that $v_2 = v_1\big|_{\Omega_2}$ and summing together $(11)_{\mathrm{I}}$–$(11)_{\mathrm{II}}$, we get (3).

Conversely, let $\tilde{u} \in H^1(\Omega)$ be the solution of Problem 1. By standard regularity results, $\tilde{u}\big|_{\Omega_i} \in H^{k+3}(\Omega_i)$, for $i = 1, 2$ [4, 21, 36]. It follows that the Γ-traces $g_1 = \tilde{u}$ and $g_2 = \nabla\tilde{u}\big|_{\Omega_1} \cdot \mathbf{n}_2$ satisfy $g_1 \in H^{k+\frac{5}{2}}(\Gamma)$ and $g_2 \in H^{k+\frac{3}{2}}(\Gamma)$. Let now $\hat{u}_1$ be the solution of the differential problem

$$\begin{cases} \mu_1\Delta^2\hat{u}_1 - \mu_1\Delta\hat{u}_1 = 0 & \text{in } \Omega_2, \\ \hat{u}_1 = g_1 & \text{on } \Gamma, \\ \nabla\hat{u}_1 \cdot \mathbf{n}_2 = g_2 & \text{on } \Gamma, \end{cases} \tag{12}$$

which reads, in weak form: find $\hat{u}_1 \in \{v \in H^2(\Omega_2)$, such that $v = g_1$ and $\nabla\hat{u}_1 \cdot \mathbf{n}_2 = g_2$ on $\Gamma\}$ such that:

$$\int_{\Omega_2} \mu_1\Delta\hat{u}_1\,\Delta\psi + \int_{\Omega_2} \mu_1\nabla\hat{u}_1 \cdot \nabla\psi = 0 \qquad \forall\psi \in H^2_0(\Omega_2). \tag{13}$$

The solution $\hat{u}_1$ exists, is unique, and by regularity results, it belongs $H^{k+3}(\Omega_2)$ [29]. We define:

$$u_2 = \tilde{u}\big|_{\Omega_2}, \qquad u_1 = \begin{cases} \tilde{u}\big|_{\Omega_1} & \text{on } \Omega_1, \\ \hat{u}_1 & \text{on } \Omega_2. \end{cases}$$

It follows that $u_2 \in H^{k+3}(\Omega_2)$, and that, thanks to $(12)_{\mathrm{II}}$–$(12)_{\mathrm{III}}$, $u_1 \in H^2(\Omega)$. Moreover, we define $z = -\mathcal{L}_1\hat{u}_1 = \mu_1\Delta\hat{u}_1 \in H^{k+1}(\Omega_2)$ and $\lambda = \nabla z \cdot \mathbf{n}_2 \in H^{k-\frac{1}{2}}(\Gamma)$. Our aim is now to prove that (u_1, u_2, z, λ) is a solution of (11).

It is easy to check that the last two equations of (11) are satisfied. To prove the remaining two equations, we notice that, by definition of z, we have $z + \mathcal{L}_1u_1 = 0$ in Ω_2. Hence, by applying the Green formula, with $v_1 \in V^1$:

$$-\int_{\Omega_2} zv_1 = \int_{\Omega_2} (\mathcal{L}_1u_1)\,v_1 = a_1^{\Omega_2}(u_1, v_1) - \langle\partial_{\mathbf{n}_2}^{\mathcal{L}_1}u_1\big|_{\Omega_2}, v_1\rangle_\Gamma. \tag{14}$$

Moreover, by applying the Green formula to (3), we have for any $v_1 \in V^1$:

$$\int_{\Omega_1} (\mathcal{L}_1u_1)\,v_1 + \langle\partial_{\mathbf{n}_1}^{\mathcal{L}_1}u_1\big|_{\Omega_1}, v_1\rangle_\Gamma + \int_{\Omega_2} (\mathcal{L}_2u_2)\,v_1 + \langle\partial_{\mathbf{n}_2}^{\mathcal{L}_2}u_2, v_1\rangle_\Gamma = \int_{\Omega_1} f_1v_1 + \int_{\Omega_2} f_2v_1.$$

By taking test functions with compact support in Ω_1, it follows $\mathcal{L}_1u_1 = f_1$ in Ω_1 the sense of distributions. Hence, by taking $v_1 \in V^1$:

$$\int_{\Omega_1} f_1v_1 = \int_{\Omega_1} (\mathcal{L}_1u_1)\,v_1 = a_1^{\Omega_1}(u_1, v_1) - \langle\partial_{\mathbf{n}_1}^{\mathcal{L}_1}u_1\big|_{\Omega_1}, v_1\rangle_\Gamma. \tag{15}$$

By summing (14) and (15), we get

$$a_1^{\Omega}(u_1, v_1) + \int_{\Omega_2} zv_1 - \langle\partial_{\mathbf{n}_2}^{\mathcal{L}_1}u_1\big|_{\Omega_2}, v_1\rangle_\Gamma - \langle\partial_{\mathbf{n}_1}^{\mathcal{L}_1}u_1\big|_{\Omega_1}, v_1\rangle_\Gamma = \int_{\Omega_1} f_1v_1. \tag{16}$$

Thanks to $(12)_{\mathrm{III}}$, the two boundary terms cancel, thus yielding $(11)_{\mathrm{I}}$. Finally, by subtracting $(11)_{\mathrm{I}}$ from (3), we get $(11)_{\mathrm{II}}$. Therefore, (u_1, u_2, z, λ) is a solution of (11). By the uniqueness of the solution of Problem 1, the solution of (11) is unique in terms of $u_1\big|_{\Omega_1}$ and u_2.

□

4.3 A-BLM/FD formulation in the general case

So far we have introduced the A-BLM/FD formulation for the Laplace equation. Let us now consider a general interface problem in the form (1). Then, the extension problem (10) generalizes to:

$$\begin{cases} \mathcal{L}_1\hat{u}_1 + z = f_1 & \text{in } \Omega_2, \\ -\Delta z + z = 0 & \text{in } \Omega_2, \end{cases} \tag{17}$$

where f_1 has been conveniently extended into Ω_2. The A-BLM/FD formulation reads as follows.

Problem 6. *Find $u_1 \in V^1$, $u_2 \in V^2$, $z \in V^2$, $\lambda \in Q$ such that*

$$
\begin{cases}
a_1^{\Omega}(u_1, v_1) + \displaystyle\int_{\Omega_2} z\, v_1 = \int_{\Omega} f_1 v_1 & \forall\, v_1 \in V^1, \\
a_2^{\Omega_2}(u_2, v_2) - a_1^{\Omega_2}(u_1, v_2) - \displaystyle\int_{\Omega_2} z\, v_2 = \int_{\Omega_2} (f_2 - f_1) v_2 & \forall\, v_2 \in V^2, \\
\displaystyle\int_{\Omega_2} \nabla z \cdot \nabla s + \int_{\Omega_2} z s = \langle \lambda, s \rangle_{\Gamma} & \forall\, s \in V^2, \\
\langle \mu, u_1 - u_2 \rangle_{\Gamma} = 0 & \forall\, \mu \in Q.
\end{cases}
\tag{18}
$$

We now show that, by formally proceeding, we recover the interface problem (1) from (18). By using (8), from $(18)_{\mathrm{I}}$ it follows

$$
\begin{aligned}
\int_{\Omega_1} (\mathcal{L}_1 u_1)\, v_1 + \int_{\Omega_2} (\mathcal{L}_1 u_1)\, v_1 + \langle \partial_{\mathbf{n}_1}^{\mathcal{L}_1} u_1\big|_{\Omega_1}, v_1 \rangle_{\Gamma} + \langle \partial_{\mathbf{n}_2}^{\mathcal{L}_1} u_1\big|_{\Omega_2}, v_1 \rangle_{\Gamma} \\
+ \langle \partial_{\mathbf{n}_1}^{\mathcal{L}_1} u_1, v_1 \rangle_{\partial\Omega} + \int_{\Omega_2} z\, v_1 = \int_{\Omega_1} f_1 v_1 + \int_{\Omega_2} f_1 v_1.
\end{aligned}
\tag{19}
$$

By taking test functions with compact support in Ω_1 and Ω_2, we get respectively

$$
\mathcal{L}_1 u_1 = f_1 \qquad \text{in } \Omega_1, \tag{20}
$$

$$
\mathcal{L}_1 u_1 + z = f_1 \qquad \text{in } \Omega_2. \tag{21}
$$

Now, combining (19)-(20)-(21), we get

$$
\begin{gathered}
\partial_{\mathbf{n}_1}^{\mathcal{L}_1} u_1\big|_{\Omega_1} + \partial_{\mathbf{n}_2}^{\mathcal{L}_1} u_1\big|_{\Omega_2} = 0 \qquad \text{on } \Gamma, \\
\partial_{\mathbf{n}_1}^{\mathcal{L}_1} u_1 = 0 \qquad \text{on } \partial\Omega.
\end{gathered}
\tag{22}
$$

Then, we apply Green formula to $(18)_{\mathrm{II}}$:

$$
\int_{\Omega_2} (\mathcal{L}_2 u_2)\, v_2 + \langle \partial_{\mathbf{n}_2}^{\mathcal{L}_2} u_2, v_2 \rangle_{\Gamma} - \int_{\Omega_2} (\mathcal{L}_1 u_1)\, v_2 - \langle \partial_{\mathbf{n}_2}^{\mathcal{L}_1} u_1\big|_{\Omega_2}, v_2 \rangle_{\Gamma} - \int_{\Omega_2} z\, v_2 = \int_{\Omega_2} (f_2 - f_1) v_2. \tag{23}
$$

By exploiting (21) and by taking test functions with compact support in Ω_2, we get

$$
\mathcal{L}_2 u_2 = f_2 \qquad \text{in } \Omega_2, \tag{24}
$$

and then

$$
\partial_{\mathbf{n}_2}^{\mathcal{L}_2} u_2 - \partial_{\mathbf{n}_2}^{\mathcal{L}_1} u_1\big|_{\Omega_2} = 0 \qquad \text{on } \Gamma, \tag{25}
$$

which, combined with (22) gives

$$
\partial_{\mathbf{n}_2}^{\mathcal{L}_2} u_2 + \partial_{\mathbf{n}_1}^{\mathcal{L}_1} u_1\big|_{\Omega_1} = 0 \qquad \text{on } \Gamma.
$$

5 Finite Element approximation

We consider a family $\mathcal{T}_h^1$ of regular meshes in Ω and a family $\mathcal{T}_h^2$ of regular meshes in Ω_2. We also introduce a family $\mathcal{T}_h^{\Gamma}$ of regular meshes for the interface Γ. One possibility, albeit not the only one, is to define $\mathcal{T}_h^{\Gamma}$ as the set of boundary faces of $\mathcal{T}_h^2$. Let us denote by h_1, h_2 and h_{Γ} the mesh element size of the three meshes. For simplicity, we consider a single parameter $h > 0$, and we assume that there exist positive constants $c_{1,1}$, $c_{2,1}$, $c_{1,2}$, $c_{2,2}$, $c_{1,\Gamma}$, $c_{2,\Gamma}$, such that

$$
c_{1,1} h \le h_1 \le c_{2,1} h, \qquad c_{1,2} h \le h_2 \le c_{2,2} h, \qquad c_{1,\Gamma} h \le h_{\Gamma} \le c_{2,\Gamma} h.
$$

We consider the Finite Element spaces $V_h^1 \subset V^1$, associated with $\mathcal{T}_h^1$, $V_h^2 \subset V^2$, associated with $\mathcal{T}_h^2$, and $Q_h \subset Q$, associated with $\mathcal{T}_h^{\Gamma}$. Then, the Finite Element counterpart of Problem 6 reads:

Problem 7. *Find $u_{h1} \in V_h^1$, $u_{h2} \in V_h^2$, $z_h \in V_h^2$, $\lambda_h \in Q_h$ such that*

$$\begin{cases} a_1^{\Omega}(u_{h1}, w_{h1}) + \int_{\Omega_2} z_h\, w_{h1} = \int_{\Omega} f_1 w_{h1} & \forall\, w_{h1} \in V_h^1, \\ a_2^{\Omega_2}(u_{h2}, w_{h2}) - a_1^{\Omega_2}(u_{h1}, w_{h2}) - \int_{\Omega_2} z_h\, w_{h2} = \int_{\Omega_2} (f_2 - f_1) w_{h2} & \forall\, w_{h2} \in V_h^2, \\ \int_{\Omega_2} \nabla z_h \cdot \nabla s_h + \int_{\Omega_2} z_h s_h = \langle \lambda_h, s_h \rangle_\Gamma & \forall\, s_h \in V_h^2, \\ \langle \mu_h, u_{h1} - u_{h2} \rangle_\Gamma = 0 & \forall\, \mu_h \in Q_h. \end{cases} \tag{26}$$

5.1 Theory of generalized saddle-point problems

To analyze Problem 7, we leverage the theory of generalized saddle-point problems [8, 43]. We report here the main results in this regard, and we refer to [8, 43] for further details.

In this section, $\mathbb{V}$ and Q denote two Hilbert spaces. Let $a\colon \mathbb{V} \times \mathbb{V} \to \mathbb{R}$ and $b_i\colon \mathbb{V} \times Q \to \mathbb{R}$, for $i = 1, 2$, be continuous bilinear forms, and $f \in \mathbb{V}^*$. The generalized saddle-point problem reads as follows.

Problem 8. *Find $u \in \mathbb{V}$, $\lambda \in Q$ such that*

$$\begin{cases} a(u, w) - b_1(w, \lambda) = {}_{\mathbb{V}^*}\langle f, w \rangle_{\mathbb{V}} & \forall\, w \in \mathbb{V}, \\ b_2(u, \mu) = 0 & \forall\, \mu \in Q. \end{cases} \tag{27}$$

Let us now consider a family of discrete spaces $\mathbb{V}_h \subset \mathbb{V}$ and $Q_h \subset Q$, and the continuous bilinear forms $a_h\colon \mathbb{V}_h \times \mathbb{V}_h \to \mathbb{R}$ and $b_h^i\colon \mathbb{V}_h \times Q_h \to \mathbb{R}$ (for $i = 1, 2$). Then, we consider the following discrete counterpart of Problem 8:

Problem 9. *Find $u_h \in \mathbb{V}_h$, $\lambda_h \in Q_h$ such that*

$$\begin{cases} a_h(u_h, w_h) - b_h^1(w_h, \lambda_h) = {}_{\mathbb{V}^*}\langle f, w_h \rangle_{\mathbb{V}} & \forall\, w_h \in \mathbb{V}_h, \\ b_h^2(u_h, \mu_h) = 0 & \forall\, \mu_h \in Q_h. \end{cases} \tag{28}$$

We define, for $i = 1, 2$, the kernels of the bilinear forms b_i and b_h^i:

$$\begin{aligned} K_i &= \mathrm{Kern}(b_i) = \{v \in \mathbb{V}\colon b_i(v, \mu) = 0 \quad \forall\, \mu \in Q\}. \\ K_h^i &= \mathrm{Kern}(b_h^i) = \{v_h \in \mathbb{V}_h\colon b_h^i(v_h, \mu_h) = 0 \quad \forall\, \mu_h \in Q_h\}. \end{aligned}$$

Notice that, in general, we do not have $K_h^i \subset K_i$. The analysis of Problem 9 is based on some hypothesis. First, we assume that, for any $h > 0$, there exists a constant $\alpha_{h,1} > 0$ such that

$$\forall\, u_h \in K_h^2 \qquad \sup_{w_h \in K_h^1} \frac{a_h(u_h, w_h)}{\|w_h\|_{\mathbb{V}}} \geq \alpha_{h,1} \|u_h\|_{\mathbb{V}}, \tag{29}$$

$$\forall\, w_h \in K_h^1 \setminus \{0\} \qquad \sup_{u_h \in K_h^2} a_h(u_h, w_h) > 0. \tag{30}$$

Moreover, we assume that, for $i = 1, 2$ and $h > 0$, there exists a constant $\beta_{h,i} > 0$ such that

$$\forall\, \mu_h \in Q_h \qquad \sup_{v_h \in \mathbb{V}_h} \frac{b_h^i(v_h, \mu_h)}{\|v_h\|_{\mathbb{V}}} \geq \beta_{h,i} \|\mu_h\|_Q \tag{31$_i$}$$

Finally, we denote by γ_h the norm of a_h:

$$\gamma_h = \sup_{u_h \in \mathbb{V}_h, v_h \in \mathbb{V}_h} \frac{a_h(u_h, u_h)}{\|u_h\|_{\mathbb{V}} \|v_h\|_{\mathbb{V}}}.$$

We have the following fundamental result.

Theorem 2. *[8, Corollary 2.2] Assume that* (29), (30), $(31)_i$ *($i = 1, 2$) hold true. Then, Problem 9 has a unique solution* (u_h, λ_h)*. Moreover,* u_h *satisfies the following stability estimate:*

$$\|u_h\|_{\mathbb{V}} \le \alpha_{h,1}^{-1}\|f\|_{\mathbb{V}^*}.$$

Moreover, we have the following convergence result.

Theorem 3. *[8, Theorem 2.2] Assume that that the hypothesis* (29) *holds. Then, the solution* (u, λ) *of Problem 8 and the solution* (u_h, λ_h) *of Problem 9 satisfy the following estimate, for some constant* $C > 0$*:*

$$\begin{aligned}\|u - u_h\|_{\mathbb{V}} \le C(1 + \alpha_{h,1}^{-1})\Bigg[&(1 + \gamma_h)\inf_{v_h \in K_h^2}\|u - v_h\|_{\mathbb{V}}\\ &+ \inf_{v_h \in \mathbb{V}_h}\left((1 + \gamma_h)\|u - v_h\|_{\mathbb{V}} + \sup_{w_h \in \mathbb{V}_h}\frac{(a - a_h)(v_h, w_h)}{\|w_h\|_{\mathbb{V}}}\right)\\ &+ \inf_{\mu_h \in Q_h}\left(\|\lambda - \mu_h\|_Q + \sup_{w_h \in \mathbb{V}_h}\frac{(b_1 - b_h^1)(w_h, \mu_h)}{\|w_h\|_{\mathbb{V}}}\right)\Bigg].\end{aligned} \tag{32}$$

The first term on the right-hand side of (32) can be estimated as follows.

Theorem 4. *[8, Proposition 2.1] Suppose that the hypothesis* $(31)_i$ *holds. then, for any* $v \in K_i$ *we have*

$$\inf_{w_h \in K_h^i}\|v - w_h\|_{\mathbb{V}} \le C(1 + \beta_{h,i}^{-1})\inf_{v_h \in \mathbb{V}_h}\left[\|v - v_h\|_{\mathbb{V}} + \sup_{\mu_h \in Q_h}\frac{(b_i - b_h^i)(v_h, \mu_h)}{\|\mu_h\|_Q}\right].$$

Clearly the optimality of the estimate (32) depends on the behavior of $\alpha_{h,1}$, $\beta_{h,i}$ and γ_h when $h \to 0$. In particular, optimality could be hindered when these constants tend to zero with h.

5.2 Analysis of the A-BLM/FD Finite Element formulation

We now go back to the analysis of Problem 7. As a matter of fact, its continuous counterpart (namely Problem 6) can be recast into the framework of generalized saddle-point problems. For this purpose, let us introduce the product space $\mathbb{V} = V^1 \times V^2$, and we write $u = (u_1, u_2) \in \mathbb{V}$. The space $\mathbb{V}$ is endowed with the norm $\|u\|_{\mathbb{V}} = (\|u_1\|_{1,\Omega}^2 + \|u_2\|_{1,\Omega_2}^2)^{1/2}$. Rewriting Problem 6 as a generalized saddle-point problem is possible by elimination of the unknown z. Let us introduce the map $\Psi\colon Q \to V^2$, such that we have $z = \Psi(\lambda)$, with $\lambda \in Q$, if and only if

$$(z, s)_{1,\Omega_2} = \langle \lambda, s\rangle_\Gamma \qquad \forall\, s \in V^2. \tag{33}$$

In other terms, z is the Riesz representative in $H^1(\Omega_2)$ of the functional $\lambda \circ \tau_\Gamma\colon V^2 \to \mathbb{R}$, namely the composition of λ with the trace operator $\tau_\Gamma\colon V^2 \to H^{1/2}(\Gamma)$.

Then, Problem 6 can be rewritten in the form of Problem 8, having defined the bilinear form $a\colon \mathbb{V}\times\mathbb{V} \to \mathbb{R}$

$$\begin{aligned}a(u, v) &= a_1^{\Omega}(u_1, v_1) + a_2^{\Omega_2}(u_2, v_2) - a_1^{\Omega_2}(u_1, v_2)\\ &= a_1^{\Omega_1}(u_1, v_1) + a_2^{\Omega_2}(u_2, v_2) + a_1^{\Omega_2}(u_1, v_1 - v_2),\end{aligned}$$

the right-hand side $f \in \mathbb{V}^*$

$$_{\mathbb{V}^*}\langle f, v\rangle_{\mathbb{V}} = \int_\Omega f_1 v_1 + \int_{\Omega_2}(f_2 - f_1)v_2,$$

and the two bilinear forms $b_i\colon \mathbb{V} \times Q \to \mathbb{R}$, for $i = 1, 2$

$$\begin{aligned}b_1(u, \lambda) &= \int_{\Omega_2}\Psi(\lambda)\,(u_1 - u_2),\\ b_2(u, \lambda) &= \langle \lambda, u_1 - u_2\rangle_\Gamma.\end{aligned}$$

Let us now move to the discrete formulation. We introduce the product space $\mathbb{V}_h = V_h^1 \times V_h^2$, and we use the notation $u_h = (u_{h1}, u_{h2}) \in \mathbb{V}_h$. Moreover, we introduce the discrete counterpart of the map Ψ, that is $\Psi_h\colon Q_h \to V_h^2$, defined so that we have $z_h = \Psi_h(\lambda_h)$, if and only if

$$(z_h, s_h)_{1,\Omega_2} = \langle \lambda_h, s_h\rangle_\Gamma \qquad \forall\, s_h \in V_h^2.$$

Then, we introduce the discrete counterpart of b_1, defined as

$$b_h^1(u_h, \lambda_h) = \int_{\Omega_2} \Psi_h(\lambda_h)\,(u_{h1} - u_{h2}).$$

Hence, it is possible to rewrite Problem 7 as follows.

Problem 10. *Find $u_h \in \mathbb{V}_h$, $\lambda_h \in Q_h$ such that*

$$\begin{cases} a(u_h, w_h) - b_h^1(w_h, \lambda_h) = {}_{\mathbb{V}^*}\langle f, w_h\rangle_{\mathbb{V}} & \forall\, w_h \in \mathbb{V}_h, \\ b_2(u_h, \mu_h) = 0 & \forall\, \mu_h \in Q_h. \end{cases}$$

Problem 10 is of course a particular case of Problem 9, where $a_h = a$ and $b_h^2 = b_2$. When it is useful to clarify the domain of definition, we will still use b_h^2 instead of b_2. We are then within the framework of Theorem 2 and Theorem 3. Therefore, in what follows we shall find conditions that ensure the hypotheses of these results.

We first consider the inf-sup condition associated with b_2. To prove this result, we assume that the pair V_h^1–Q_h is inf-sup stable, in the sense of the Ladyzhenskaya-Babuška-Brezzi (LBB) condition [10], that is there exists $C > 0$, independent of h, such that

$$\forall\, \mu_h \in Q_h \setminus \{0\} \qquad \sup_{w_{h1} \in V_h^1} \frac{\langle \mu_h, w_{h1}\rangle_\Gamma}{\|w_{h1}\|_{1,\Omega}\|\mu_h\|_{-\frac{1}{2},\Gamma}} \geq C. \tag{34}$$

Examples of pairs V_h^1–Q_h satisfying the inf-sup condition (34) have been widely studied in the literature [6, 22, 28, 32]. Typically, (34) holds true under a condition of the type $h_1 \leq K\, h_\Gamma$ (for some constant $K > 0$). Then, we have the following result.

Lemma 5. *Suppose that the pair V_h^1–Q_h is inf-sup stable (i.e.* (34) *holds true). There exists $\beta_2 > 0$ such that*

$$\forall\, \mu_h \in Q_h \setminus \{0\} \qquad \sup_{w_h \in \mathbb{V}_h} \frac{b_2(w_h, \mu_h)}{\|w_h\|_{\mathbb{V}}\|\mu_h\|_{-\frac{1}{2},\Gamma}} \geq \beta_2. \tag{35}$$

Proof. The thesis follows by restricting the sup on the subset $w_h = (w_{h1}, 0)$. □

We then consider the inf-sup condition associated with b_h^1. As will become apparent later, for the purpose of proving convergence of the solution u_h, in $(31)_i$ we need not have $\beta_{h,1}$ independent of h. This translates into weaker assumptions. Specifically, we assume that the pair V_h^2–Q_h satisfies the kernel condition

$$\forall\, \mu_h \in Q_h \setminus \{0\} \quad \exists\, w_{h2} \in V_h^2 \qquad \langle \mu_h, w_{h2}\rangle_\Gamma > 0. \tag{36}$$

This condition on the pair V_h^2–Q_h is weaker than the inf-sup stability that we have assumed for the pair V_h^1–Q_h (see (34)). Indeed, examples of pairs V_h^2–Q_h satisfying the kernel condition (36) are easily obtained by taking Q_h to be the space of traces of V_h^2 or a subset of the latter.

Moreover, on the space V_h^2, we assume the inverse inequality

$$\forall\, w_{h1} \in V_h^2 \qquad \|\nabla w_{h1}\|_{0,\Omega_2} \leq C_I h_1^{-1} \|w_{h1}\|_{0,\Omega_2}, \tag{37}$$

for some constant $C_I > 0$.

Lemma 6. *Suppose that the pair V_h^2–Q_h satisfies the kernel condition* (36)*, and that the inverse inequality* (37) *holds on the space V_h^2. Then, for any $h > 0$, there exists $\beta_{h,1} > 0$ such that*

$$\forall\, \mu_h \in Q_h \setminus \{0\} \qquad \sup_{w_h \in \mathbb{V}_h} \frac{b_h^1(w_h, \mu_h)}{\|w_h\|_{\mathbb{V}}\|\mu_h\|_{-\frac{1}{2},\Gamma}} \geq \beta_{h,1}. \tag{38}$$

Proof. The application $S_h\colon Q_h \to (V_h^2)^*$ defined as

$$_{(V_h^2)^*}\langle S_h\mu_h, w_{h2}\rangle_{V_h^2} = \langle \mu_h, w_{h2}\rangle_\Gamma$$

is injective by (36). Hence, the inverse of S_h is well-defined on its image and, since Q_h is finite dimensional, it is bounded. It follows that there exists a constant $C_h > 0$, possibly dependent of h, such that

$$\|\mu_h\|_{-\frac{1}{2},\Gamma} \le C_h \|S_h\mu_h\|_{(V_h^2)^*} = C_h \sup_{w_{h2}\in V_h^2} \frac{\langle \mu_h, w_{h2}\rangle_\Gamma}{\|w_{h2}\|_{1,\Omega_2}}.$$

By definition of Ψ_h, for any $w_{h2} \in V_h^2$, we have

$$\langle \mu_h, w_{h2}\rangle_\Gamma = \int_{\Omega_2} \nabla\Psi_h(\mu_h)\cdot\nabla w_{h2} + \int_{\Omega_2} \Psi_h(\mu_h)\, w_{h2} = (\Psi_h(\mu_h), w_{h2})_{1,\Omega_2}\,.$$

Clearly, the supremum

$$\sup_{w_{h2}\in V_h^2} \frac{(\Psi_h(\mu_h), w_{h2})_{1,\Omega_2}}{\|w_{h2}\|_{1,\Omega_2}}$$

is attained for $w_{h2} = \Psi_h(\mu_h)$. It follows

$$\|\mu_h\|_{-\frac{1}{2},\Gamma} \le C_h\|\Psi_h(\mu_h)\|_{1,\Omega_2} \le C_h(1 + C_I^2 h_2^{-2})\frac{\|\Psi_h(\mu_h)\|_{0,\Omega_2}^2}{\|\Psi_h(\mu_h)\|_{1,\Omega_2}},$$

where we have used the inverse inequality (37). Finally, we bound the right-hand side as follows

$$\begin{aligned}
\|\mu_h\|_{-\frac{1}{2},\Gamma} &\le C_h(1 + C_I^2 h_2^{-2}) \sup_{w_{h2}\in V_h^2} \frac{\int_{\Omega_2}\Psi_h(\mu_h) w_{h2}}{\|w_{h2}\|_{1,\Omega_2}}\\
&\le C_h(1 + C_I^2 h_2^{-2}) \sup_{w_h\in \mathbb{V}_h} \frac{\int_{\Omega_2}\Psi_h(\mu_h)\,(u_{h1} - u_{h2})}{\|w_{h2}\|_{1,\Omega_2}}\\
&= C_h(1 + C_I^2 h_2^{-2}) \sup_{w_h\in \mathbb{V}_h} \frac{b_h^1(w_h,\mu_h)}{\|w_h\|_{\mathbb{V}}}.
\end{aligned}$$

□

Concerning the discrete inf-sup condition for a, we assume that the constant $\alpha_{h,1}$ does not depend of h, that is to say there exists a constant $\alpha_1 > 0$ such that

$$\forall\, u_h \in K_h^2 \qquad \sup_{w_h\in K_h^1} \frac{a(u_h, w_h)}{\|w_h\|_{\mathbb{V}}} \ge \alpha_1\|u_h\|_{\mathbb{V}}. \tag{39}$$

This condition clearly depends on the particular interface problem considered, as it involves the bilinear forms a_1 and a_2. Hence, at this stage, we keep (39) as an assumption. We will address this topic again in Section 5.3.

Finally, we assume that there exists a constant $\gamma > 0$ such that

$$\forall\, u_h \in \mathbb{V}_h,\ v_h \in \mathbb{V}_h \qquad a(u_h, u_h) \le \gamma\|u_h\|_{\mathbb{V}}\|v_h\|_{\mathbb{V}} \tag{40}$$

This is an immediate consequence of the continuity of the original bilinear forms a_1 and a_2. We are now ready to state and prove the main result.

Theorem 7. *Suppose that the pair V_h^2–Q_h satisfies the kernel condition* (36)*, the pair V_h^1–Q_h satisfies the inf-sup condition* (34)*, and that the inverse inequality* (37) *holds on the space V_h^2. Moreover, assume that* (39) *and* (40) *hold true. Then, Problem 7 admits a unique solution $(u_{h1}, u_{h2}, z, \lambda_h)$. Moreover, there exists a constant $C > 0$, independent of h, such that, if (u_1, u_2, z, λ) is a solution of Problem 6, we have*

$$\begin{aligned}
\|u_1 - u_{h1}\|_{1,\Omega} + \|u_2 - u_{h2}\|_{1,\Omega_2} \le C\Big[&\inf_{v_{h1}\in V_h^1}\|u_1 - v_{h1}\|_{1,\Omega} + \inf_{v_{h2}\in V_h^2}\|u_2 - v_{h1}\|_{1,\Omega_2}\\
&+ \inf_{\mu_h\in Q_h}\|\lambda - \mu_h\|_{-\frac{1}{2},\Gamma} + \inf_{s_h\in V_h^2}\|z - s_h\|_{1,\Omega_2}\Big]
\end{aligned} \tag{41}$$

Proof. By Lemma 6 and Lemma 5, the kernels of the transpose of b_h^1 and b_h^2 are trivial, that is $\mathrm{Kern}((b_h^i)^T) = \{0\}$ for $i = 1, 2$. Hence, we have $\dim K_h^1 = \dim K_h^2$ [10, Cor. 3.1.2], that is equivalent, in finite dimension, to (30) [8, Eq. (2.21)]. Therefore, thanks also to Lemma 6 and to Lemma 5, all the hypotheses of Theorem 3 are satisfied. By combining Theorem 4 with Theorem 3, we have:

$$\begin{aligned}\|u-u_h\|_{\mathbb{V}} \le C(1+\alpha_1^{-1})\Bigg[&(1+\gamma)(2+\beta_2^{-1})\inf_{v_h\in\mathbb{V}_h}\|u-v_h\|_{\mathbb{V}}\\ &+\inf_{\mu_h\in Q_h}\left(\|\lambda-\mu_h\|_{-\frac{1}{2},\Gamma}+\sup_{w_h\in\mathbb{V}_h}\frac{(b_1-b_h^1)(w_h,\mu_h)}{\|w_h\|_{\mathbb{V}}}\right)\Bigg].\end{aligned}$$

We now estimate the term involving $b_1 - b_h^1$:

$$\begin{aligned}(b_1-b_h^1)(w_h,\mu_h) &= \int_{\Omega_2}\left(\Psi(\mu_h)-\Psi_h(\mu_h)\right)(w_{h1}-w_{h2})\\ &\le \|\Psi(\mu_h)-\Psi_h(\mu_h)\|_{0,\Omega_2}\|w_{h1}-w_{h2}\|_{0,\Omega_2}.\end{aligned}$$

We notice that

$$\|w_{h1}-w_{h2}\|_{0,\Omega_2} \le \|w_{h1}\|_{1,\Omega}+\|w_{h2}\|_{1,\Omega_2} \le \left(2\|w_{h1}\|_{1,\Omega}^2+2\|w_{h2}\|_{1,\Omega_2}^2\right)^{1/2} = \sqrt{2}\|w_h\|_{\mathbb{V}}.$$

Moreover, by the Céa Lemma

$$\begin{aligned}\|\Psi(\mu_h)-\Psi_h(\mu_h)\|_{1,\Omega_2} &\le \inf_{s_h\in V_h^2}\|\Psi(\mu_h)-s_h\|_{1,\Omega_2}\\ &\le \inf_{s_h\in V_h^2}\|\Psi(\mu_h)-\Psi(\lambda)+\Psi(\lambda)-s_h\|_{1,\Omega_2}\\ &\le \|\Psi(\mu_h)-\Psi(\lambda)\|_{1,\Omega_2}+\inf_{s_h\in V_h^2}\|\Psi(\lambda)-s_h\|_{1,\Omega_2}.\end{aligned}$$

By standard arguments, from (33) it follows that

$$\|\Psi(\mu_h)-\Psi(\lambda)\|_{1,\Omega_2} \le C_{\mathrm{tr}}\|\mu_h-\lambda\|_{-\frac{1}{2},\Gamma},$$

where we have used the trace inequality

$$\forall v_2\in V^2 \qquad \|v_2\|_{1/2,\Gamma} \le C_{\mathrm{tr}}\|v_2\|_{1,\Omega_2}.$$

Hence

$$\begin{aligned}&\inf_{\mu_h\in Q_h}\left(\|\lambda-\mu_h\|_{-\frac{1}{2},\Gamma}+\sup_{w_h\in\mathbb{V}_h}\frac{(b_1-b_h^1)(w_h,\mu_h)}{\|w_h\|_{\mathbb{V}}}\right)\\ &\quad\le \inf_{\mu_h\in Q_h}\left(\|\lambda-\mu_h\|_{-\frac{1}{2},\Gamma}+\sqrt{2}\left(C_{\mathrm{tr}}\|\mu_h-\lambda\|_{-\frac{1}{2},\Gamma}+\inf_{s_h\in V_h^2}\|\Psi(\lambda)-s_h\|_{1,\Omega_2}\right)\right)\\ &\quad\le (1+\sqrt{2}C_{\mathrm{tr}})\inf_{\mu_h\in Q_h}\|\lambda-\mu_h\|_{-\frac{1}{2},\Gamma}+\sqrt{2}\inf_{s_h\in V_h^2}\|\Psi(\lambda)-s_h\|_{1,\Omega_2}.\end{aligned}$$

Therefore, recalling that $\Psi(\lambda) = z$, we have

$$\begin{aligned}\|u-u_h\|_{\mathbb{V}} \le C(1+\alpha_1^{-1})\Bigg[&(1+\gamma)(2+\beta_2^{-1})\inf_{v_h\in\mathbb{V}_h}\|u-v_h\|_{\mathbb{V}}\\ &+(1+\sqrt{2}C_{\mathrm{tr}})\inf_{\mu_h\in Q_h}\|\lambda-\mu_h\|_{-\frac{1}{2},\Gamma}+\sqrt{2}\inf_{s_h\in V_h^2}\|z-s_h\|_{1,\Omega_2}\Bigg].\end{aligned}$$

Finally, the thesis follows by noticing that

$$\inf_{v_h\in\mathbb{V}_h}\|u-v_h\|_{\mathbb{V}} \le \inf_{v_{h1}\in V_h^1}\|u_1-v_{h1}\|_{1,\Omega}+\inf_{v_{h2}\in V_h^2}\|u_2-v_{h1}\|_{1,\Omega_2}.$$

$\square$

Remark 2. Apparently, the convergence estimate (41) is not significantly different than the estimate (6) and, in a sense, they are both *optimal*. The big difference is played by the behavior for $h \to 0$ of the term

$$\inf_{v_{h1} \in V_h^1} \|u_1 - v_{h1}\|_{1,\Omega}.$$

Indeed, if u_1 is not regular (as for the DLM/FD and BLM/FD formulations), the convergence rate is typically low. The A-BLM/FD method, instead, thanks to the higher global regularity of u_1 achieves faster convergence rates.

5.3 A numerical test for the condition (39)

Among the assumptions of Theorem 7, the only one we have not yet analyzed thus far is condition (39). First, we notice that this condition can be equivalently rewritten in the inf-sup form

$$\inf_{u_h \in K_h^2} \sup_{w_h \in K_h^1} \frac{a(u_h, w_h)}{\|w_h\|_{\mathbb{V}} \|u_h\|_{\mathbb{V}}} \geq \alpha_1.$$

Here and in the rest of the paper, we implicitly assume that the inf is taken by excluding $u_h = 0$, which would make the argument undefined. We notice that, for standard point-saddle problems (i.e., when $b_1 = b_2$ and $b_h^1 = b_h^2$), such inf-sup condition is a consequence of the uniform coercivity of a on the kernel $K_h^1 = K_h^2$, or, a fortiori, on the whole space $\mathbb{V}_h$. For generalized point-saddle problems, however, the uniform coercivity of a does not imply the inf-sup condition (39), since the two arguments u_h and w_h must be taken in different spaces, K_h^2 and K_h^1 respectively (unless $K_h^2 \subseteq K_h^1$, but this condition is not met in our case).

Unlike for the conditions (35) and (38), the validity of the condition (39) depends on the interface problem at hand (and thus on the form of a_1 and a_2), as well as on the choice of spaces V_h^1, V_h^2 and Q_h. In this section, we illustrate a test that allows one to perform, for a specific interface problem and for a choice of spaces V_h^1, V_h^2 and Q_h, a numerical verification of the validity of the condition (39).

Let us denote by $n_i = \dim V_h^i$ the dimension of the Finite Element subspaces of V^i, for $i = 1, 2$. We then introduce $n_u = \dim \mathbb{V}_h = n_1 + n_2$ and $n_q = \dim Q_h$. In what follows, we use bold symbols to denote the algebraic counterparts of Finite Element functions. Specifically, we denote by $\mathbf{u}_i \in \mathbb{R}^{n_i}$ the vector collecting the degrees of freedom associated with u_{hi}, for $i = 1, 2$, and by $\mathbf{u} = (\mathbf{u}_1, \mathbf{u}_2) \in \mathbb{R}^{n_u}$ the algebraic counterpart of $u_h = (u_{h1}, u_{h2}) \in \mathbb{V}_h$. Similarly, we denote by $\boldsymbol{\mu} \in \mathbb{R}^{n_q}$ the vector collecting the degrees of freedom associated with μ_h. We introduce then the matrices $\mathsf{A}_h \in \mathbb{R}^{n_u \times n_u}$ and $\mathsf{B}_h^i \in \mathbb{R}^{n_u \times n_q}$, the algebraic counterparts of the bilinear forms a and b_i, for $i = 1, 2$, respectively, defined through the relationships

$$a(u_h, w_h) = \mathbf{w}^T \mathsf{A}_h \mathbf{u}, \qquad b_h^1(u_h, \mu_h) = \boldsymbol{\mu}^T \mathsf{B}_h^1 \mathbf{u}, \qquad b_2(u_h, \mu_h) = \boldsymbol{\mu}^T \mathsf{B}_h^2 \mathbf{u},$$

for any $u_h, w_h \in \mathbb{V}_h$ and $\mu_h \in Q_h$. Moreover, we define the matrix $\mathsf{N}_h \in \mathbb{R}^{n_u \times n_u}$

$$\mathsf{N}_h = \begin{pmatrix} \mathsf{M}_h^1 + \mathsf{K}_h^1 & \\ & \mathsf{M}_h^2 + \mathsf{K}_h^2 \end{pmatrix}^{\frac{1}{2}},$$

where $\mathsf{M}_h^i \in \mathbb{R}^{n_i \times n_i}$ and $\mathsf{K}_h^i \in \mathbb{R}^{n_i \times n_i}$ are the mass and stiffness matrices, respectively, associated with V_h^i for $i = 1, 2$. The matrix N_h allows us to relate the $\mathbb{V}$-norm of u_h with its algebraic counterpart $\mathbf{u}$:

$$\|u_h\|_{\mathbb{V}} = \|\mathsf{N}_h \mathbf{u}\|_2,$$

where $\|\cdot\|_2$ denotes the euclidean norm.

To derive an algebraic counterpart of condition (39) that is easy to verify in practice, we perform two steps. First, we represent the solution in a new coordinate system, namely by $\widetilde{\mathbf{u}} = \mathsf{N}_h \mathbf{u} \in \mathbb{R}^{n_u}$, so that $\|\widetilde{\mathbf{u}}\|_2 = \|u_h\|_{\mathbb{V}}$. In this coordinate system, the operators a and b_i, for $i = 1, 2$, are associated with the matrices $\widetilde{\mathsf{A}}_h = \mathsf{N}_h^{-T} \mathsf{A}_h \mathsf{N}_h^{-1}$ and $\widetilde{\mathsf{B}}_h^i = \mathsf{B}_h^i \mathsf{N}_h^{-1}$, respectively.

Second, we restrict the action of a_h to $K_h^2 \times K_h^1 \subset \mathbb{V}_h \times \mathbb{V}_h$. For this purpose, for $i = 1, 2$, let $\boldsymbol{\Psi}_h^i \in \mathbb{R}^{n_u \times (n_u - n_q)}$ be a matrix whose columns are an orthonormal basis of Kern $\widetilde{\mathsf{B}}_h^i$. In practice, the matrix $\boldsymbol{\Psi}_h^i$ can be obtained by extracting the last $n_u - n_q$ columns from V, where $\mathsf{U}\Sigma\mathsf{V}^T = \widetilde{\mathsf{B}}_h^i$ is the singular value decomposition of $\widetilde{\mathsf{B}}_h^i$. With the help of $\boldsymbol{\Psi}_h^i$, we perform a second change of coordinates, and we write, for $i = 1, 2$, elements of $\operatorname{Kern} \widetilde{\mathsf{B}}_h^i$ as $\widetilde{\mathbf{u}} = \boldsymbol{\Psi}_h^i \widehat{\mathbf{u}}$, where $\widehat{\mathbf{u}} \in \mathbb{R}^{n_u - n_q}$. We remark that, being the columns of $\boldsymbol{\Psi}_h^i$ orthonormal, this transformation preserves the norm, that is $\|\widehat{\mathbf{u}}\|_2 = \|\widetilde{\mathbf{u}}\|_2 = \|u_h\|_{\mathbb{V}}$.

In summary, $u_h \in K_h^i = \operatorname{Kern} b_h^i$ if and only if $\mathbf{u} \in \operatorname{Kern} \mathsf{B}_h^i$, that is equivalent to the condition $\mathbf{u} = \mathsf{N}_h^{-1} \boldsymbol{\Psi}_h^i \widehat{\mathbf{u}}$ for some $\widehat{\mathbf{u}} \in \mathbb{R}^{n_u - n_q}$. If follows that

$$
\begin{aligned}
\inf_{u_h \in K_h^2} \sup_{w_h \in K_h^1} \frac{a(u_h, w_h)}{\|w_h\|_{\mathbb{V}} \|u_h\|_{\mathbb{V}}} &= \inf_{\widehat{\mathbf{u}} \in \mathbb{R}^{n_u - n_q}} \sup_{\widehat{\mathbf{w}} \in \mathbb{R}^{n_u - n_q}} \frac{\left(\mathsf{N}_h^{-1} \boldsymbol{\Psi}_h^1 \widehat{\mathbf{w}}\right)^T \mathsf{A}_h \left(\mathsf{N}_h^{-1} \boldsymbol{\Psi}_h^2 \widehat{\mathbf{u}}\right)}{\|\boldsymbol{\Psi}_h^2 \widehat{\mathbf{u}}\|_2 \|\boldsymbol{\Psi}_h^1 \widehat{\mathbf{w}}\|_2} \\
&= \inf_{\widehat{\mathbf{u}} \in \mathbb{R}^{n_u - n_q}} \sup_{\widehat{\mathbf{w}} \in \mathbb{R}^{n_u - n_q}} \frac{\widehat{\mathbf{w}}^T \widehat{\mathsf{A}}_h \widehat{\mathbf{u}}}{\|\widehat{\mathbf{u}}\|_2 \|\widehat{\mathbf{w}}\|_2},
\end{aligned}
\tag{42}
$$

where we have defined the matrix $\widehat{\mathsf{A}}_h \in \mathbb{R}^{(n_u - n_q) \times (n_u - n_q)}$ as

$$
\widehat{\mathsf{A}}_h = (\boldsymbol{\Psi}_h^1)^T \mathsf{N}_h^{-T} \mathsf{A}_h \mathsf{N}_h^{-1} \boldsymbol{\Psi}_h^2.
$$

We have thus rephrased condition (39), that involves the interaction between the bilinear form a and the kernels of b_h^1 and b_h^2, into an algebraic conditions involving a single algebraic object, that is the matrix $\widehat{\mathsf{A}}_h$. Remarkably, the right-hand side of (42) coincides with the lowest singular value of $\widehat{\mathsf{A}}_h$, that we denote by $\sigma_{\min}(\widehat{\mathsf{A}}_h)$. In conclusion, condition (39) can be equivalently rewritten as: there exists a constant $\alpha_1 > 0$, such that, for any $h > 0$

$$
\sigma_{\min}(\widehat{\mathsf{A}}_h) \geq \alpha_1.
$$

In practice, to test whether condition (39) holds true for a particular interface problem and for a particular triplet of Finite Element spaces V_h^1, V_h^2 and Q_h, we shall consider meshes of increasing refinements, and look at the trend of $\sigma_{\min}(\widehat{\mathsf{A}}_h)$. In the case of $\sigma_{\min}(\widehat{\mathsf{A}}_h) \to 0$ when $h \to 0$, then condition (39) will not be verified; if, on the other hand, $\sigma_{\min}(\widehat{\mathsf{A}}_h)$ shows to be bounded from below by a constant, then condition (39) will be deemed valid (at least for the range of h used, which in practice is most often what is needed).

This test, albeit not being a demonstration, makes it possible to test quickly and easily whether or not the Finite Element spaces chosen may constitute a good choice, in the spirit of other similar tests used in the literature [20].

6 Numerical results

In this section we present some numerical tests in a two-dimensional domain, aimed at verifying the theoretical results of this paper and at comparing the proposed method with existing ones.

6.1 Problem setting

We consider $\Omega \subset \mathbb{R}^2$ to be the open unit square centered in the origin, and we define Ω_2 as a circular domain with radius 0.3 centered in the origin as well (see Fig. 2). We consider the following differential problem:

$$
\begin{cases}
-\mu_1 \Delta \tilde{u}_1 + \tilde{u}_1 = f & \text{in } \Omega_1, \\
-\mu_2 \Delta \tilde{u}_2 + \tilde{u}_2 = f & \text{in } \Omega_2, \\
\tilde{u}_1 = \tilde{u}_2 & \text{on } \Gamma, \\
\mu_1 \nabla \tilde{u}_1 \cdot \mathbf{n}_1 + \mu_2 \nabla \tilde{u}_2 \cdot \mathbf{n}_2 = 0 & \text{on } \Gamma, \\
\mu_1 \nabla \tilde{u}_1 \cdot \mathbf{n}_1 = 0 & \text{on } \partial\Omega,
\end{cases}
\tag{43}
$$

with the forcing term $f(x, y) = \sin(\pi x) + \tanh(y)$. In the following sections, we consider different values for the pair (μ_1, μ_2). Specifically, we consider four cases, namely $(10, 1)$, $(2, 1)$, $(1, 2)$, and $(1, 10)$. We identify each case through the ratio $\mu_2/\mu_1 \in \{0.1, 0.5, 2, 10\}$.

For the numerical approximation of (43), we consider and compare the following methods (see Table 1 for a summary).

Method	**Weak formulation**	**Unknowns**	**Mesh**
FEM-fit	Problem 1	$\tilde{u} \in V^1 = H^1_{0,\Gamma_D}(\Omega)$	$\mathcal{T}_h^{\mathrm{fit}}$
FEM-unfit	Problem 1	$\tilde{u} \in V^1 = H^1_{0,\Gamma_D}(\Omega)$	$\mathcal{T}_h^1$
DLM/FD-diag DLM/FD-tria	Problem 2	$u_1 \in V^1 = H^1_{0,\Gamma_D}(\Omega)$ $u_2 \in V^2 = H^1(\Omega_2)$ $p \in (H^1(\Omega_2))^*$	$\mathcal{T}_h^1$ $\mathcal{T}_h^2$ $\mathcal{T}_h^2$
BLM/FD	Problem 4	$u_1 \in V^1 = H^1_{0,\Gamma_D}(\Omega)$ $u_2 \in V^2 = H^1(\Omega_2)$ $\lambda \in Q = H^{-1/2}(\Gamma)$	$\mathcal{T}_h^1$ $\mathcal{T}_h^2$ $\mathcal{T}_h^\Gamma$
A-BLM/FD	Problem 6	$u_1 \in V^1 = H^1_{0,\Gamma_D}(\Omega)$ $u_2 \in V^2 = H^1(\Omega_2)$ $\lambda \in Q = H^{-1/2}(\Gamma)$ $z \in V^2 = H^1(\Omega_2)$	$\mathcal{T}_h^1$ $\mathcal{T}_h^2$ $\mathcal{T}_h^\Gamma$ $\mathcal{T}_h^2$

Table 1: Numerical methods considered in this work. For each method we report the corresponding weak formulation, the unknowns of the weak formulation and the computational mesh used for their discretization.

- The standard Finite Element formulation based on Problem 1. In this case, we will consider either a computational mesh that is fitted to Γ (called $\mathcal{T}_h^{\mathrm{fit}}$) or an unfitted mesh (namely $\mathcal{T}_h^1$). We will refer to the two methods as **FEM-fit** and **FEM-unfit**, respectively.
- The Finite Element formulation of Problem 2. As anticipated in Section 3.1, the first term of $(4)_{\mathrm{II}}$ can be set equal either to $a_2^{\Omega_2}(u_2, v_2)$ or to $a_2^{\Omega_2}(u_1, v_2)$. The corresponding matrix A_h is, respectively, block diagonal and block lower-triangular. For this reason, we will refer to the two methods as **DLM/FD-diag** and **DLM/FD-tria**, respectively.
- The Finite Element formulation of Problem 4, called **BLM/FD** method.
- Our proposed **A-BLM/FD** method (see Problem 7).

Among the six methods compared, the FEM-fit method benefits from an advantage, as it is built on a mesh fitted to the interface Γ. Therefore, we consider it as a benchmark, since it allows us to give an indication of the error that would be possible to obtain, for a given differential problem and mesh resolution, with a fitted method. We then assess how the five unfitted methods perform, in comparison with FEM-fit.

We consider regular triangular meshes $\mathcal{T}_h^{\mathrm{fit}}$, $\mathcal{T}_h^1$ and $\mathcal{T}_h^2$ with different resolutions. For the four FD methods considered (namely DLM/FD-diag, DLM/FD-tria, BLM/FD, A-BLM/FD), we investigate the impact of the ratio h_2/h_1 (we consider three cases: $h_2/h_1 \in \{0.5, 1, 2\}$). We define the interface mesh $\mathcal{T}_h^\Gamma$ as the union of the boundary segments of $\mathcal{T}_h^2$. Example of computational meshes are reported in Fig. 2.

To define the spaces V_h^1, V_h^2, Λ_h, we focus in this work on P1 and P2 continuous Finite Elements defined on the corresponding meshes. For the space Q_h, we consider globally continuous piecewise polynomials defined on $\mathcal{T}_h^\Gamma$ with order either 1 (P1 elements) or 2 (P2 elements). For simplicity, we only consider the case of equal order spaces, namely either P1/P1/P1 elements or P2/P2/P2, with reference to the three spaces used (that is $V_h^1/V_h^2/\Lambda_h$ for the DLM/FD-diag and DLM/FD-tria methods; $V_h^1/V_h^2/Q_h$ for the BLM/FD and A-BLM/FD methods).

6.2 Numerical verification of condition (39)

In this section, we apply the test described in Section 5.3 to the example problem (43), to numerically check condition (39). Specifically, we consider meshes with increasing resolution. For each combination of $\mu_2/\mu_1 \in \{0.1, 0.5, 2, 10\}$ and of $h_2/h_1 \in \{0.5, 1, 2\}$, we assemble the matrix $\widehat{\mathsf{A}}_h$ and we compute its minimum singular value $\sigma_{\min}(\widehat{\mathsf{A}}_h)$. Finally, we plot the trend of $\sigma_{\min}(\widehat{\mathsf{A}}_h)$ with respect to h.

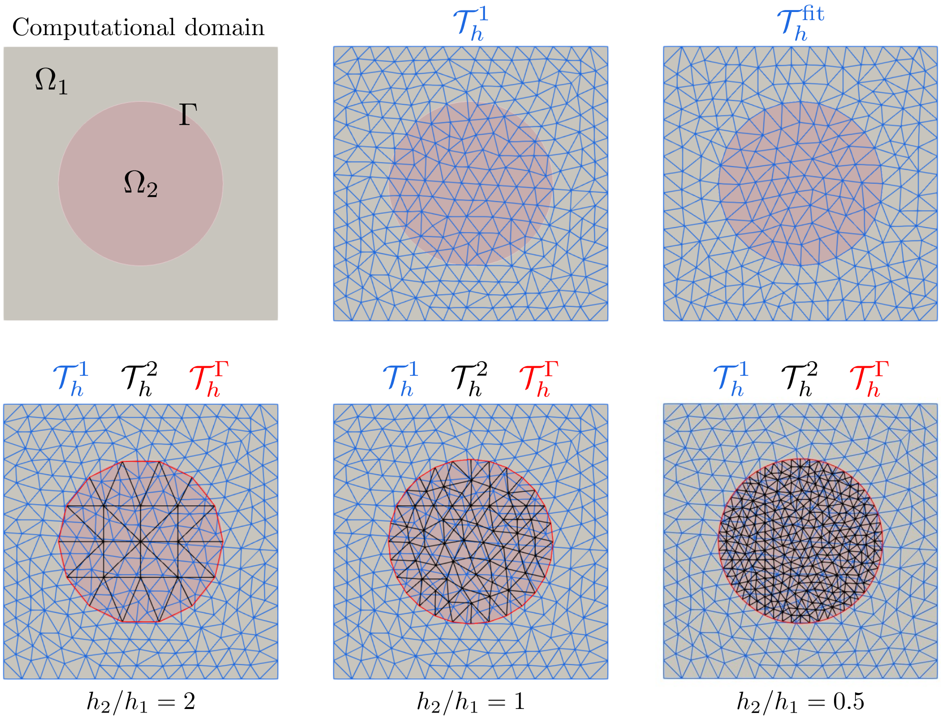

Figure 2: Computational domain and some examples of computational meshes. First line: computational domain; mesh $\mathcal{T}_h^1$ (used in the FEM-unfit method); mesh $\mathcal{T}_h^{\text{fit}}$ (used in the FEM-fit method). In the second line, we show the three meshes $\mathcal{T}_h^1$, $\mathcal{T}_h^2$ and $\mathcal{T}_h^\Gamma$ for three different values of h_2/h_1 (reported below).

The results are reported in Fig. 3, both for P1/P1/P1 elements and P2/P2/P2 elements. In the case $\mu_2/\mu_1 < 1$ with P1/P1/P1 elements, the test is clearly passed, since $\sigma_{\min}(\widehat{\mathsf{A}}_h)$ is virtually constant with respect to h, for every choice of μ_2/μ_1 and for every choice of h_2/h_1. In the other cases the value of $\sigma_{\min}(\widehat{\mathsf{A}}_h)$ is more variable; still, in almost all the cases, despite the small fluctuations, $\sigma_{\min}(\widehat{\mathsf{A}}_h)$ do not show a decreasing trend. The only exceptions occur in the case $\mu_2/\mu_1 > 1$ with P1/P1/P1 elements, where, for some values of h_2/h_1, a decreasing trend is noticeable, albeit with a rather low rate (approximately between $h^{1/4}$ and $h^{1/2}$). Nevertheless, the results suggest that, provided a sufficiently large h_2/h_1 ratio is chosen, it is possible to obtain a lower bounded $\sigma_{\min}(\widehat{\mathsf{A}}_h)$ also in the case $\mu_2/\mu_1 > 1$.

6.3 Comparison of numerical solutions

In Fig. 4 we report the numerical solutions obtained, for P1 elements and with a very fine mesh (210 elements per side of the square, and a ratio $h_2/h_1 = 1$), using the different numerical methods. As the figure clearly shows, the different FD methods considered in this paper are based on a different type of solution extension to the subdomain Ω_2. In particular, the two DLM/FD (DLM/FD-tria and DLM/FD-diag) methods extend $\tilde{u}_1$ to the whole Ω in a way that is coincident to $\tilde{u}_2$. In this way, the solution u_1 inherits the gradient jumps of the solution $\tilde{u}$, which clearly emerge from the figure near the interface Γ, where we observe the contour lines breaking. We notice that, the higher the ratio μ_2/μ_1, the more pronounced are the discontinuities. Also the solution u_1 obtained by the BLM/FD method is irregular near the interface Γ, and has even more pronounced gradient discontinuities than for the DLM/FD methods. In contrast, as expected, the A-BLM/FD formulation yields a smooth u_1, as seen from the contour lines that cross the Γ interface without being bent. We notice that the largest differences between the u_1 obtained by the three methods occur (for this test case) in the case $\mu_2/\mu_1 > 1$, that is in the case for which the gradients of the $\tilde{u}$ solution have larger jumps. This will have consequences when we evaluate the errors of the numerical solutions.

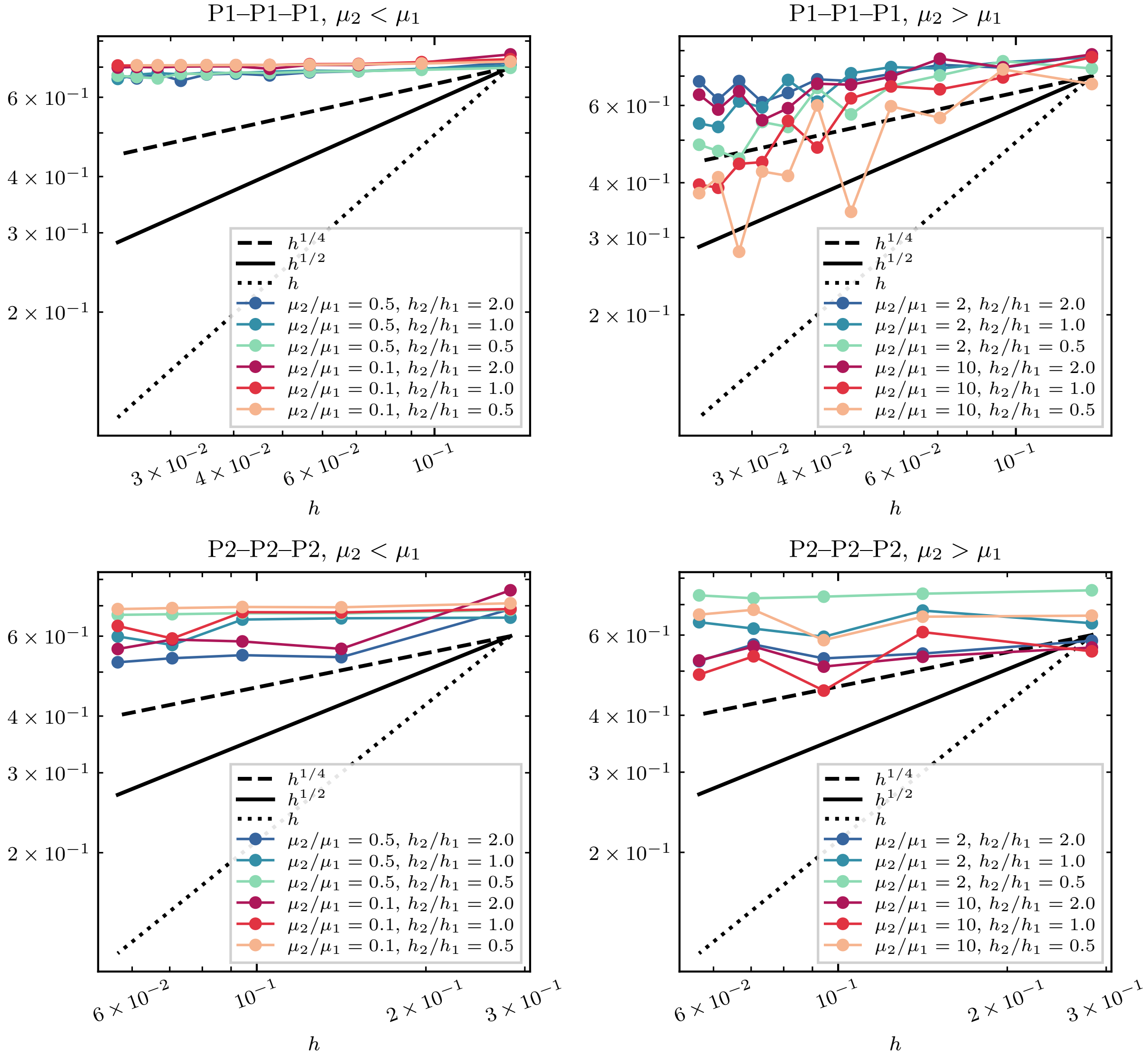

Figure 3: Minimum singular value of the matrix $\widehat{\mathsf{A}}_h$ as a function of h. Each column corresponds to a different ratio μ_2/μ_1, each row to a different polynomial order (see titles).

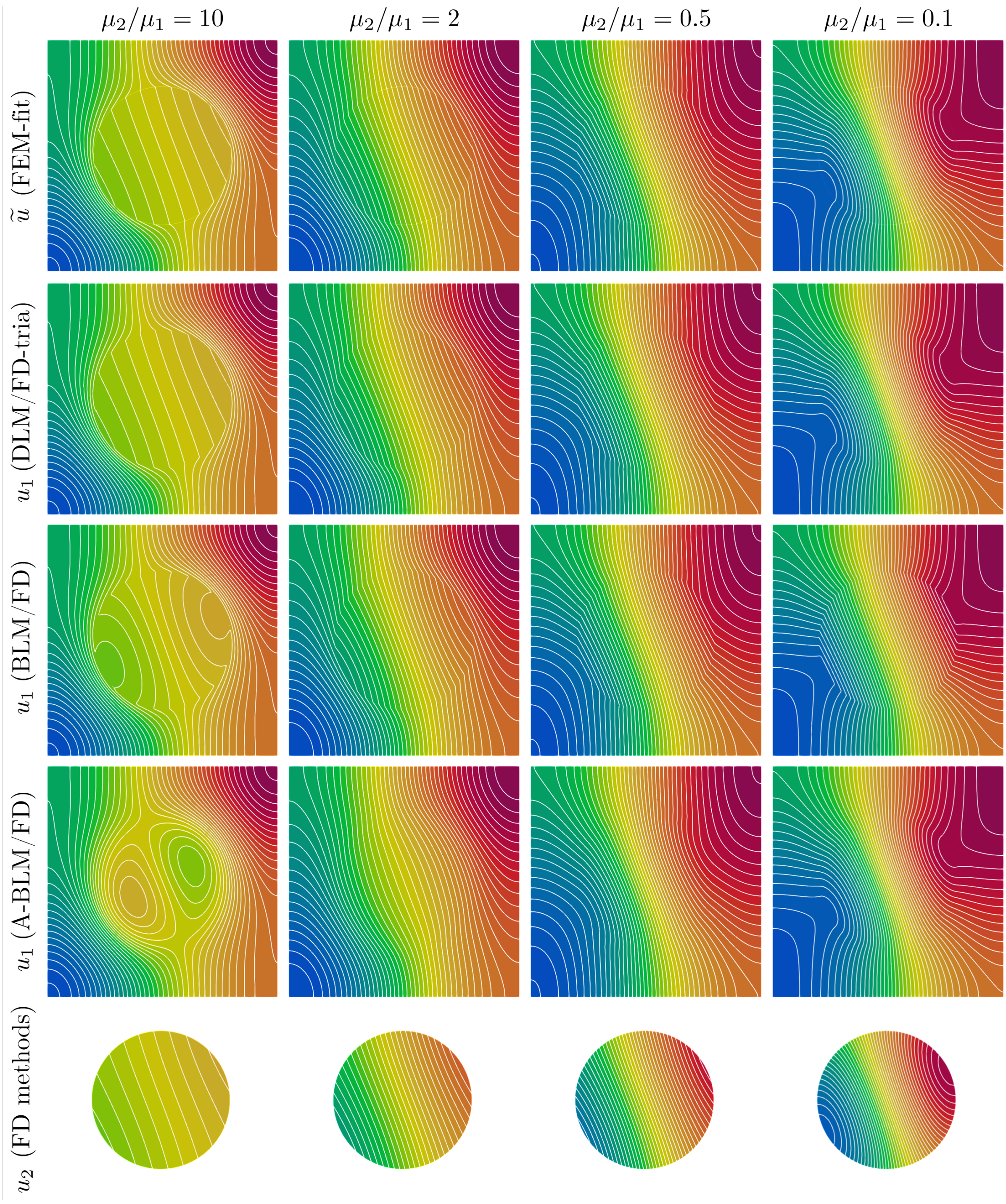

Figure 4: Numerical solutions to (43) obtained, using different numerical methods, with P1 elements on a very fine mesh (210 elements per side of the square, and a ratio $h_2/h_1 = 1$). White lines are contour lines. Each column corresponds to a different ratio μ_2/μ_1, reported on top. In the first line, we show the solution $\tilde{u}$ obtained with the FEM-fit method. We do not report the solution obtained with the FEM-unfit method, as it is very similar to that of the FEM-fit method (at least for very fine meshes). The second line reports the solution u_1 obtained with the DLM/FD-tria method. The solution obtained with the DLM/FD-diag method is conceptually similar to the latter, even if in some cases it exhibits spurious oscillations, as shown later. In the third and fourth line we show the solution u_1 obtained with the BLM/FD and A-BLM/FD methods, respectively. Finally, in the last line we show the solution u_2 obtained with the A-BLM/FD method. We do not report the solution u_2 obtained with the other FD methods, as it is virtually coincident with the latter.

6.4 Convergence tests

To numerically test the accuracy and convergence of the different methods, we consider the errors, in L^2 and H^1 norm, with respect to a reference solution obtained through the FEM-fit method on a much finer mesh. All errors reported in this work are normalized with respect to the solution norm.

Let us first consider the case of elements of order 1 (P1 for the FEM-fit and FEM-unfit methods, P1/P1/P1 for the four FD methods). The trend of the errors in norm H^1 and L^2 is shown in Fig. 5 and Fig. 6, respectively. First, we observe that, as expected, the FEM-fit method shows an optimal convergence rate (namely linear in H^1 norm and quadratic in L^2 norm). The FEM-unfit method, instead, because of the low global regularity of the solution ($\tilde{u} \in H^s(\Omega)$ with $s \in (1, 3/2)$ [4]), features a limited convergence rate (we observe order 1/2 in H^1 norm and order 1 in L^2 norm). Because of the low-regularity of the extension of $\tilde{u}_1$, the DLM/FD-tria, DLM/FD-diag and BLM/FD methods exhibit the same convergence order as the FEM-unfit method. Finally, concerning the A-BLM/FD method, the numerical tests confirm the theoretical results of this work: thanks to the underlying smooth extension, we recover optimal convergence rates.

Special attention should be given to the case of $\mu_2/\mu_1 = 0.1$. First, we notice that, in this case, the DLM/FD-diag method exhibits oscillations in the error trend and, for $h_2/h_1 \geq 1$, no convergence of the error is observed. As a matter of fact, as shown in Fig. 7, spurious oscillations are present in the numerical solution. This is not surprising, as – to the best of our knowledge – the ellipticity on the discrete kernel for the DLM/FD-diag method has been proven only in the case $\mu_2/\mu_1 > 1$ [3]. Second, we observe that, in the case $\mu_2/\mu_1 = 0.1$, the numerical errors obtained with the FEM-unfit and DLM/FD-tria are surprisingly small (even smaller than those of the A-BLM/FD method). This is due to the fact that, as it is apparent from Fig. 4, the solution of the full problem $\tilde{u}$ is "less irregular" than in the other cases (gradient jumps are less pronounced). This leads to low-magnitude errors and a faster convergence rate in the pre-asymptotic regime; nonetheless, for $h \to 0$, the error curve bends and approaches the suboptimal order $h^{1/2}$ in H^1 norm and h in L^2 norm. The errors obtained with the BLM/FD method are much larger in magnitude, because of the low regularity of the solution (see again Fig. 4), and the observed convergence rates are suboptimal. The A-BLM/FD method, instead, achieves the optimal convergence rates.

In Fig. 8 and Fig. 9, we show the errors, in H^1 and L^2 norm respectively, obtained by using second order Finite Elements. We recall that the solution u_1 has regularity $H^s(\Omega)$ with $s \in (1, 3/2)$ for the DLM/FD-tria, DLM/FD-diag, BLM/FD methods; with $s \in (2, 5/2)$ for the A-BLM/FD method. Therefore, in the energy norm H^1 we can expect at most order 3/2 for the A-BLM/FD method, and 1/2 for the other FD methods. Numerical results confirm these expectations, in the case $\mu_2/\mu_1 > 1$. The case $\mu_2/\mu_1 < 1$ requires, as for P1 Finite Elements, a more careful analysis. First, we again observe the non-convergence of the DLM/FD-diag method, if μ_2/μ_1 is sufficiently small and/or h_2/h_1 are sufficiently large. This time, the DLM/FD-tria method also exhibits similar issues, albeit in a less pronounced way. Finally, the A-BLM/FD method shows a slight reduction in the order of convergence, approaching order 1 (still higher than the order 1/2 observed for the other unfitted methods). Regarding the error in norm L^2, we observe, notwithstanding some fluctuation, that the A-BLM/FD method achieves convergence of order 2 like the benchmark FEM-fit method, while all other unfitted methods exhibit convergence of order 1.

We complement our analysis by considering different boundary conditions on the outer frontier $\partial\Omega$, to test the generality of the observations made. In particular, we consider the case of Dirichlet boundary conditions $\tilde{u}_1 = \sin(\pi x) + \tanh(y)$ on $\partial\Omega$. In Fig. 10 and Fig. 11, we show the errors obtained by using Finite Elements of order 1, in H^1 and L^2 norm, respectively. Looking at the figures, we can draw the same conclusions as in the case of Neumann boundary conditions. In particular, the A-BLM/FD method exhibits optimal convergence rate in both norms and in all cases considered, while all other unfitted methods feature a suboptimal convergence rate. The advantage of the A-BLM/FD method over the other unfitted methods in terms of error magnitude is even more pronounced tha with Neumann boundary conditions, also in the case $\mu_2/\mu_1 = 10$.

Thus far we have compared the methods by considering the errors as a function of mesh size h. However, given the same mesh size h, the different methods have different numbers of unknowns (see Table 1). In particular, the proposed A-BLM/FD method is the one with the largest number of unknowns. Compared to the DLM/FD methods, which have one unknown defined on $\mathcal{T}_h^1$ and two defined on $\mathcal{T}_h^2$, the A-BLM/FD method has one more unknown defined on $\mathcal{T}_h^\Gamma$. Nonetheless, the latter mesh, being associated with a domain of codimension 1, typically possesses a much smaller number of elements than $\mathcal{T}_h^1$ and $\mathcal{T}_h^2$, which are of

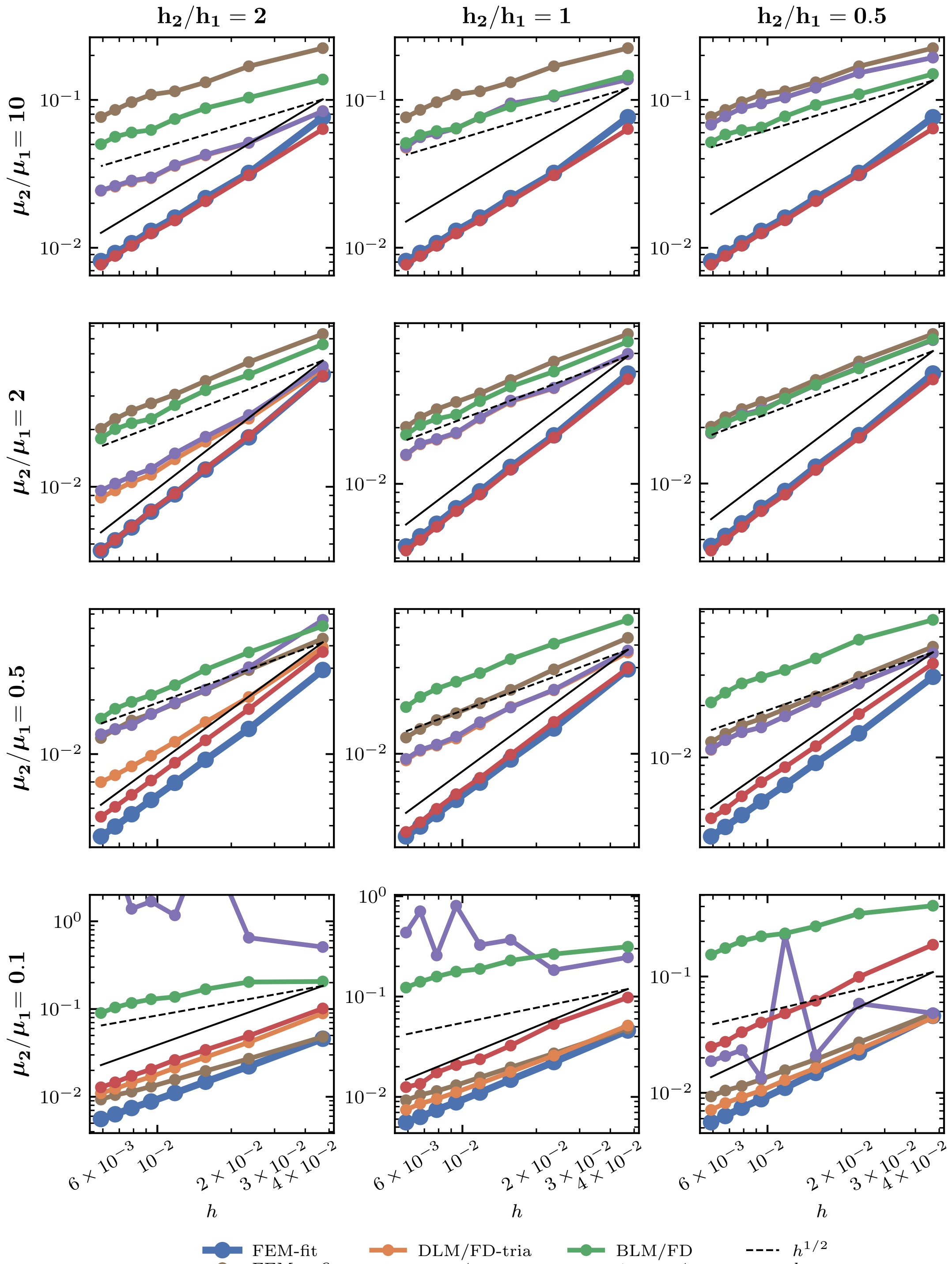

Figure 5: Relative errors in H^1 norm versus h, obtained for problem (43) with Finite Elements of order 1 with the six different numerical methods considered in this work (see legend). Each column corresponds to a different ratio h_2/h_1, reported on top. Each row corresponds to a different ratio μ_2/μ_1, reported on the left.

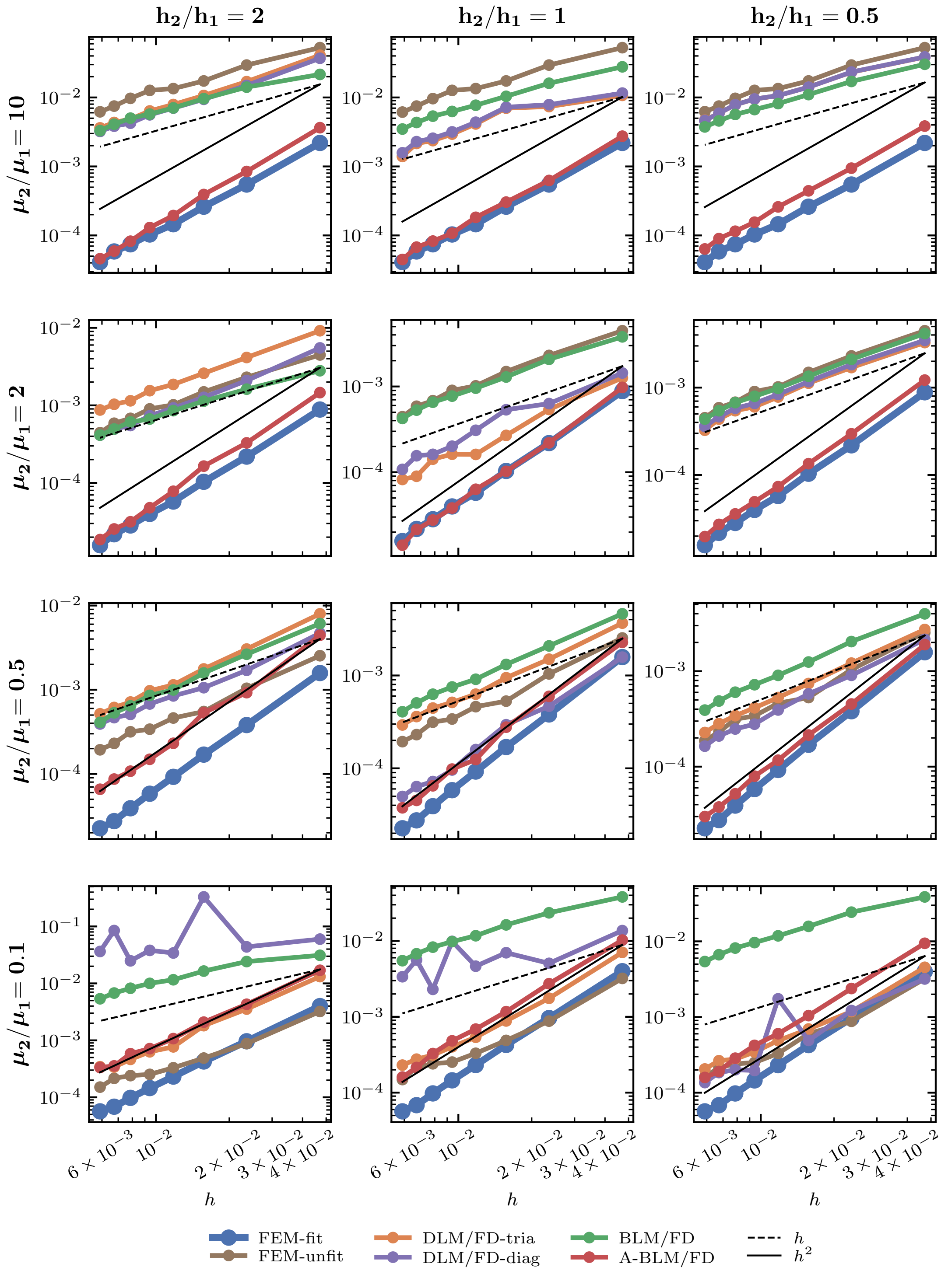

Figure 6: Relative errors in L^2 norm versus h, obtained for problem (43) with Finite Elements of order 1 with the six different numerical methods considered in this work (see legend). Each column corresponds to a different ratio h_2/h_1, reported on top. Each row corresponds to a different ratio μ_2/μ_1, reported on the left.

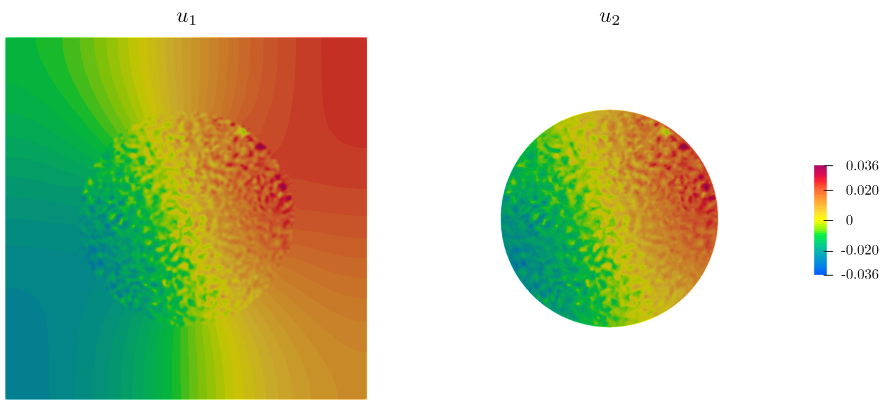

Figure 7: Numerical solution obtained through the DLM/FD-diag method for $\mu_2/\mu_1 = 0.1$, $h_2/h_1 = 2$, P1 elements on a grid with 240 element per edge of Ω.

codimension 0. To perform a quantitative analysis, we consider the error versus the total number of degrees of freedom (N_{dof}), instead of versus the mesh size h. For the sake of brevity, we report only the H^1 errors for Finite Elements of order 1, for $\mu_2/\mu_1 \in \{0.5, 2\}$ and $h_2/h_1 \in \{0.5, 1, 2\}$ (see Fig. 12). As can be seen from the figure, despite the slightly higher number of degrees of freedom than for the other FD methods, the A-BLM/FD method, thanks to the higher order of convergence, achieves higher accuracy in the considered tests not only for a given h, but also for a given N_{dof}.

7 Conclusions

We have proposed a new FD method for interface problems that allows to achieve higher convergence rates than standard FD methods. The proposed method extends the solution into the fictitious domain in a smoother way than existing FD methods do, thus improving accuracy of the Finite Element approximation, even with meshes that are not fitted to the interface. This is achieved thanks to a novel weak formulation in which the subdomain coupling is enforced neither through an $H^{-1}(\Omega_2)$ duality (as for the DLM/FD method) nor through a $H^{-1/2}(\Gamma)$ duality (as for the BLM/FD method), but through an $L^2(\Omega_2)$ product with an additional regular distributed field. In this manner, no gradient discontinuity is introduced in the analytical solution. Specifically, the additional distributed field is the H^1 Riesz representative of the BLM that enforces the solution continuity across the interface.

We have analyzed, by leveraging the theory of generalized saddle-point problems [8, 43], the well-posedness of the proposed FD formulation, thus proving an optimal error estimate. The result is based on a discrete inf-sup condition that depends on the interface problem at hand. To test the validity of the latter condition in a purely computational manner, we have proposed a test that consists in computing the lowest singular value of a suitable matrix, for increasing mesh refinements.

Numerical test, performed on a model problem with a simple geometry, confirm the theoretical results, thus showing that the proposed method allows to improve the convergence rate of standard FD approaches when the solution of the original problem is regular enough.

Acknowledgements

This project have been partially supported by the GNCS, “Gruppo Nazionale per il Calcolo Scientifico” (National Group for Scientific Computing) of INdAM (Istituto Nazionale di Alta Matematica), under the INdAM GNCS Project CUP_E55F22000270001. The present research has been partially supported by MUR, grant Dipartimento di Eccellenza 2023-2027.

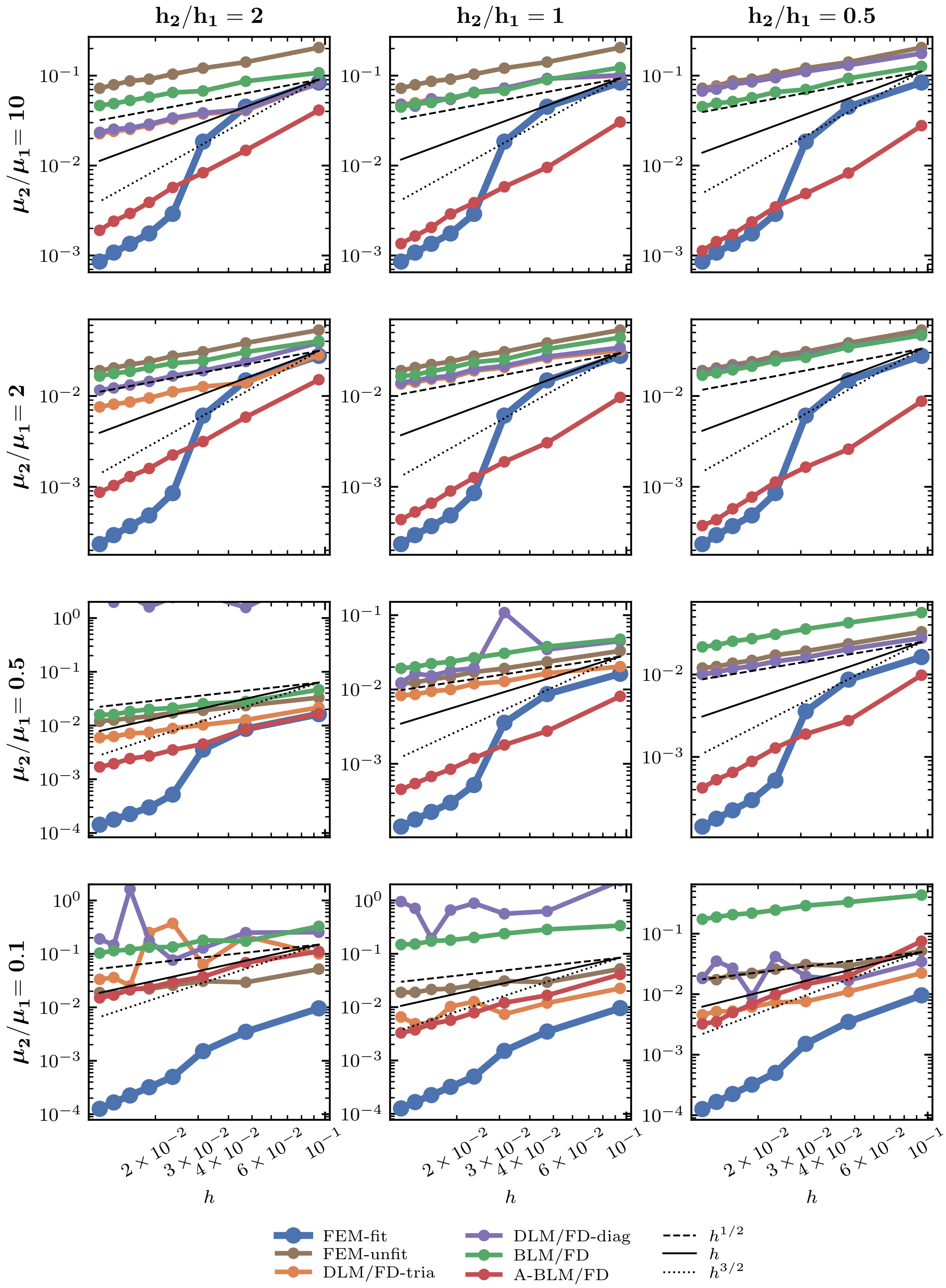

Figure 8: Relative errors in H^1 norm versus h, obtained for problem (43) with Finite Elements of order 2 with the six different numerical methods considered in this work (see legend). Each column corresponds to a different ratio h_2/h_1, reported on top. Each row corresponds to a different ratio μ_2/μ_1, reported on the left.

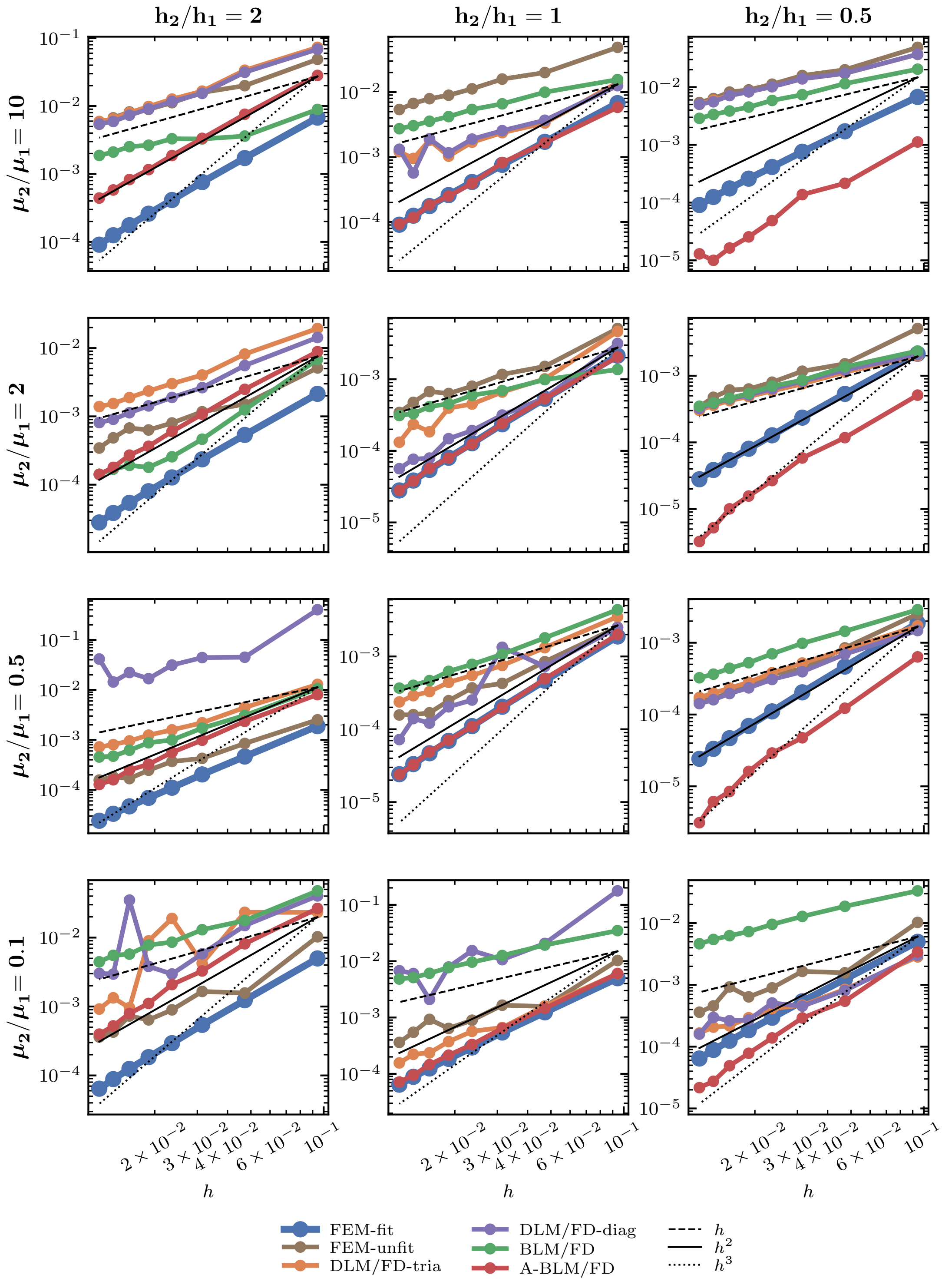

Figure 9: Relative errors in L^2 norm versus h, obtained for problem (43) with Finite Elements of order 2 with the six different numerical methods considered in this work (see legend). Each column corresponds to a different ratio h_2/h_1, reported on top. Each row corresponds to a different ratio μ_2/μ_1, reported on the left.

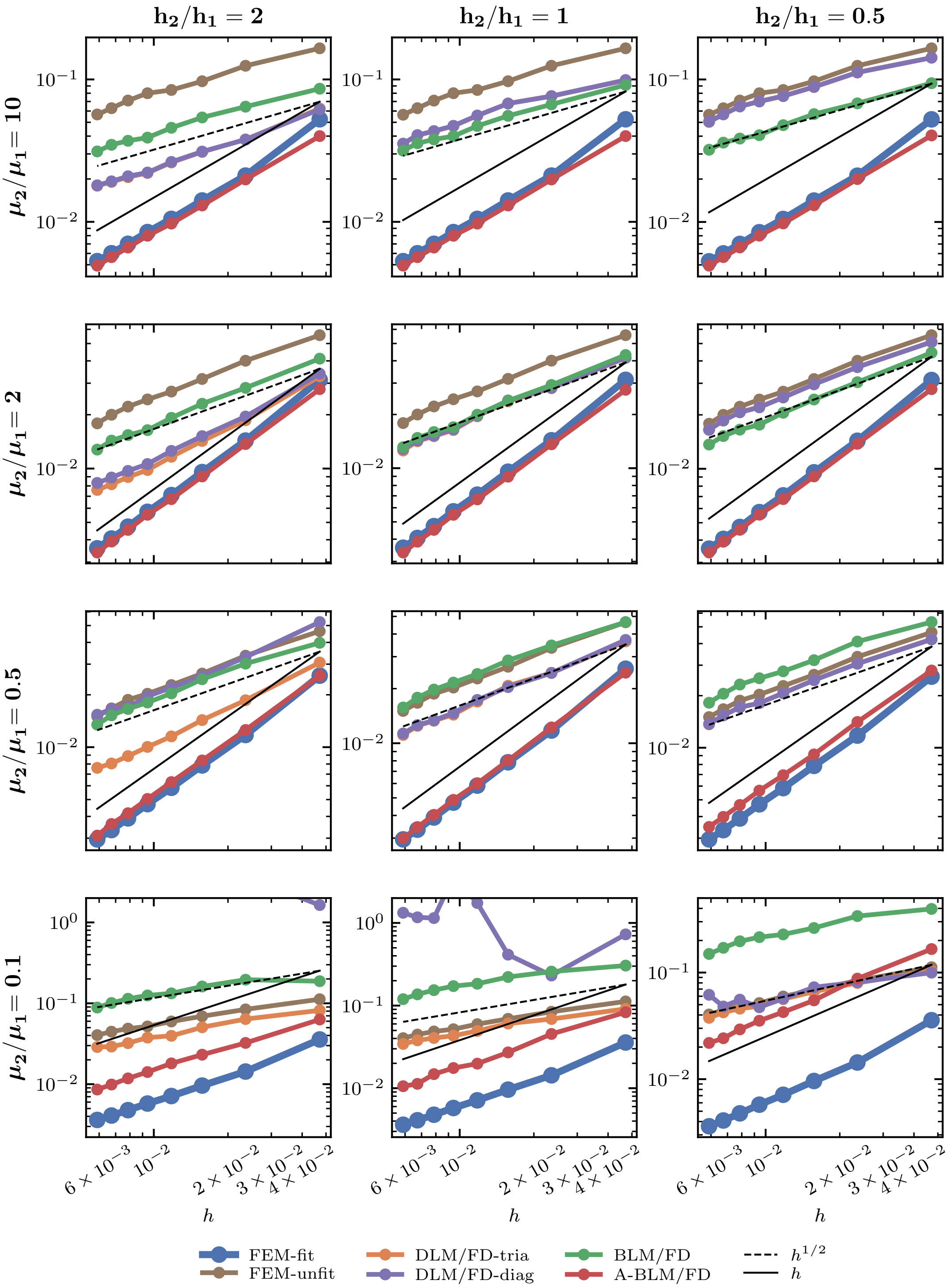

Figure 10: Relative errors in H^1 norm versus h, obtained for problem (43) with Dirichlet boundary conditions on the external boundary $\partial\Omega$, with Finite Elements of order 1 with the six different numerical methods considered in this work (see legend). Each column corresponds to a different ratio h_2/h_1, reported on top. Each row corresponds to a different ratio μ_2/μ_1, reported on the left.

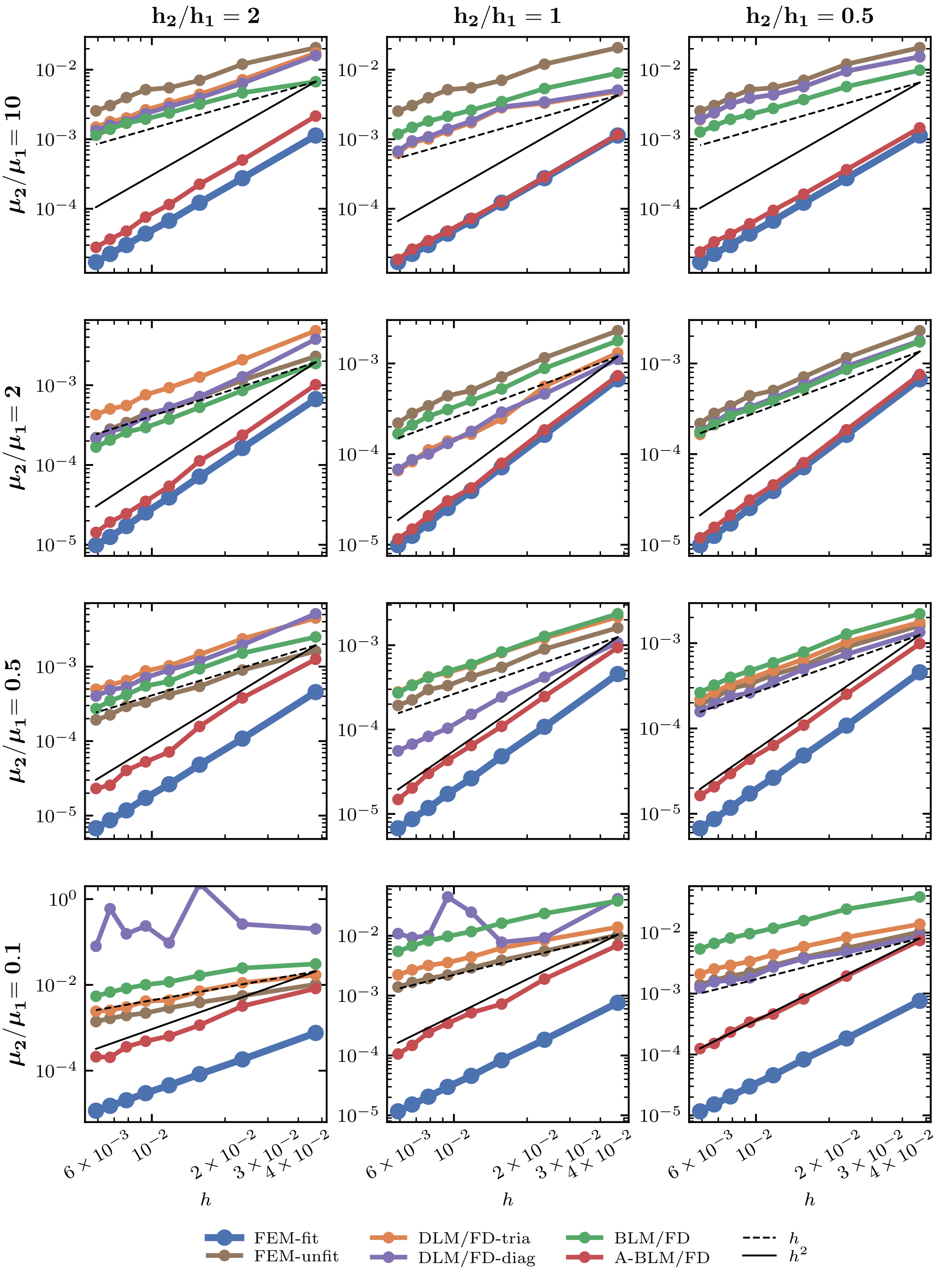

Figure 11: Relative errors in L^2 norm versus h, obtained for problem (43) with Dirichlet boundary conditions on the external boundary $\partial\Omega$, with Finite Elements of order 1 with the six different numerical methods considered in this work (see legend). Each column corresponds to a different ratio h_2/h_1, reported on top. Each row corresponds to a different ratio μ_2/μ_1, reported on the left.

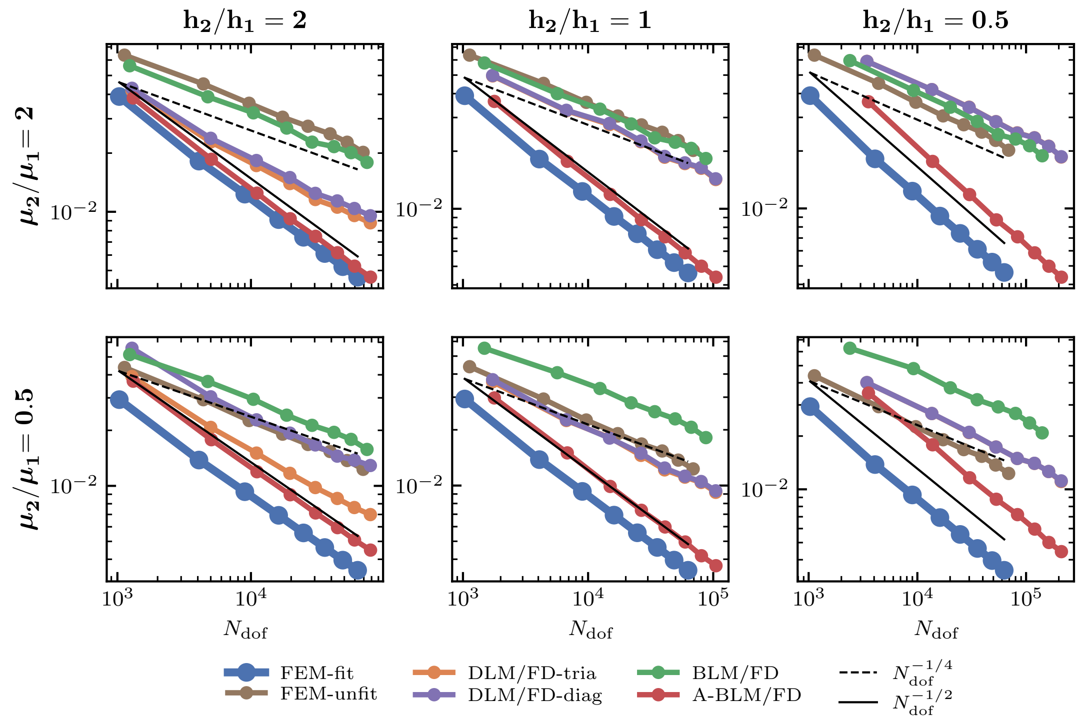

Figure 12: Relative errors in H^1 norm versus N_{dof}, obtained for problem (43) with Finite Elements of order 1 with the six different numerical methods considered in this work (see legend). Each column corresponds to a different ratio h_2/h_1, reported on top. Each row corresponds to a different ratio μ_2/μ_1, reported on the left.

References

[1] F. Alauzet, B. Fabrèges, M. A. Fernández, and M. Landajuela. "Nitsche-XFEM for the coupling of an incompressible fluid with immersed thin-walled structures". In: *Computer Methods in Applied Mechanics and Engineering* 301 (2016), pp. 300–335.

[2] F. Auricchio, D. Boffi, L. Gastaldi, A. Lefieux, and A. Reali. "A study on unfitted 1D finite element methods". In: *Computers & Mathematics with Applications* 68.12 (2014).

[3] F. Auricchio, D. Boffi, L. Gastaldi, A. Lefieux, and A. Reali. "On a fictitious domain method with distributed Lagrange multiplier for interface problems". en. In: *Applied Numerical Mathematics* 95 (2015), pp. 36–50.

[4] I. Babuška. "The finite element method for elliptic equations with discontinuous coefficients". In: *Computing* 5.3 (1970), pp. 207–213.

[5] I. Babuška. "The finite element method with Lagrangian multipliers". In: *Numerische Mathematik* 20.3 (1973), pp. 179–192.

[6] H. J. Barbosa and T. J. Hughes. "The finite element method with Lagrange multipliers on the boundary: circumventing the Babuška-Brezzi condition". In: *Computer Methods in Applied Mechanics and Engineering* 85.1 (1991), pp. 109–128.

[7] T. Belytschko and J. M. Kennedy. "Computer models for subassembly simulation". In: *Nuclear Engineering and Design* 49.1-2 (1978), pp. 17–38.

[8] C. Bernardi, C. Canuto, and Y. Maday. "Generalized Inf-Sup Conditions for Chebyshev Spectral Approximation of the Stokes Problem". en. In: *SIAM Journal on Numerical Analysis* 25.6 (1988), pp. 1237–1271.

[9] S. Berrone, A. Bonito, R. Stevenson, and M. Verani. "An optimal adaptive fictitious domain method". In: *Mathematics of Computation* 88.319 (2019), pp. 2101–2134.

[10] D. Boffi, F. Brezzi, and M. Fortin. *Mixed Element Methods and Applications*. en. Vol. 44. Springer Series in Computational Mathematics. Berlin, Heidelberg: Springer Berlin Heidelberg, 2013.

[11] D. Boffi, N. Cavallini, and L. Gastaldi. "Finite element approach to immersed boundary method with different fluid and solid densities". In: *Mathematical Models and Methods in Applied Sciences* 21.12 (2011), pp. 2523–2550.

[12] D. Boffi, N. Cavallini, and L. Gastaldi. "The finite element immersed boundary method with distributed Lagrange multiplier". In: *SIAM Journal on Numerical Analysis* 53.6 (2015), pp. 2584–2604.

[13] D. Boffi and L. Gastaldi. "A fictitious domain approach with Lagrange multiplier for fluid-structure interactions". In: *Numerische Mathematik* 135 (2017), pp. 711–732.

[14] D. Boffi and L. Gastaldi. "A finite element approach for the immersed boundary method". In: *Computers & structures* 81.8-11 (2003), pp. 491–501.

[15] J. H. Bramble. "The Lagrange multiplier method for Dirichlet's problem". In: *Mathematics of Computation* 37.155 (1981), pp. 1–11.

[16] J. H. Bramble and J. T. King. "A finite element method for interface problems in domains with smooth boundaries and interfaces". In: *Advances in Computational Mathematics* 6 (1996), pp. 109–138.

[17] M. Bucelli, A. Zingaro, P. C. Africa, I. Fumagalli, L. Dede', and A. Quarteroni. "A mathematical model that integrates cardiac electrophysiology, mechanics, and fluid dynamics: Application to the human left heart". In: *International Journal for Numerical Methods in Biomedical Engineering* 39.3 (2023), e3678.

[18] E. Burman, S. Claus, P. Hansbo, M. G. Larson, and A. Massing. "CutFEM: discretizing geometry and partial differential equations". In: *International Journal for Numerical Methods in Engineering* 104.7 (2015), pp. 472–501.

[19] E. Burman and P. Hansbo. "Fictitious domain finite element methods using cut elements: I. A stabilized Lagrange multiplier method". In: *Computer Methods in Applied Mechanics and Engineering* 199.41-44 (2010), pp. 2680–2686.

[20] D. Chapelle and K.-J. Bathe. “The inf-sup test”. In: *Computers & Structures* 47.4-5 (1993), pp. 537–545.

[21] Z. Chen and J. Zou. “Finite element methods and their convergence for elliptic and parabolic interface problems”. In: *Numerische Mathematik* 79.2 (1998), pp. 175–202.

[22] W. Dahmen and A. Kunoth. “Appending boundary conditions by Lagrange multipliers: Analysis of the LBB condition”. en. In: *Numerische Mathematik* 88.1 (2001), pp. 9–42.

[23] J. Dolbow and I. Harari. “An efficient finite element method for embedded interface problems”. In: *International Journal for Numerical Methods in Engineering* 78.2 (2009), pp. 229–252.

[24] L. C. Evans. *Partial Differential Equations*. Vol. 19. American Mathematical Society, 2022.

[25] M. Feistauer and V. Sobotíková. “Finite element approximation of nonlinear elliptic problems with discontinuous coefficients”. In: *ESAIM: Mathematical Modelling and Numerical Analysis* 24.4 (1990), pp. 457–500.

[26] T.-P. Fries and T. Belytschko. “The extended/generalized finite element method: an overview of the method and its applications”. In: *International Journal for Numerical Methods in Engineering* 84.3 (2010), pp. 253–304.

[27] A. Gerstenberger and W. A. Wall. “An extended finite element method/Lagrange multiplier based approach for fluid–structure interaction”. In: *Computer Methods in Applied Mechanics and Engineering* 197.19-20 (2008), pp. 1699–1714.

[28] V. Girault and R. Glowinski. “Error analysis of a fictitious domain method applied to a Dirichlet problem”. In: *Japan Journal of Industrial and Applied Mathematics* 12 (1995), pp. 487–514.

[29] V. Girault and P.-A. Raviart. *Finite element methods for Navier-Stokes equations: theory and algorithms*. Vol. 5. Springer Science & Business Media, 2012.

[30] R. Glowinski and Y. Kuznetsov. “Distributed Lagrange multipliers based on fictitious domain method for second order elliptic problems”. In: *Computer Methods in Applied Mechanics and Engineering* 196.8 (2007), pp. 1498–1506.

[31] R. Glowinski, T.-W. Pan, T. I. Hesla, and D. D. Joseph. “A distributed Lagrange multiplier/fictitious domain method for particulate flows”. In: *International Journal of Multiphase Flow* 25.5 (1999), pp. 755–794.

[32] R. Glowinski, T.-W. Pan, and J. Periaux. “A fictitious domain method for Dirichlet problem and applications”. en. In: *Computer Methods in Applied Mechanics and Engineering* 111.3-4 (1994), pp. 283–303.

[33] A. Hansbo and P. Hansbo. “An unfitted finite element method, based on Nitsche’s method, for elliptic interface problems”. In: *Computer methods in applied mechanics and engineering* 191.47-48 (2002), pp. 5537–5552.

[34] C. W. Hirt, A. A. Amsden, and J. Cook. “An arbitrary Lagrangian-Eulerian computing method for all flow speeds”. In: *Journal of computational physics* 14.3 (1974), pp. 227–253.

[35] M. A. Hyman. “Non-iterative numerical solution of boundary-value problems”. In: *Applied Scientific Research, Section B* 2.1 (1952), pp. 325–351.

[36] R. Kellogg. “Singularities in interface problems”. In: *Numerical Solution of Partial Differential Equations–II*. Elsevier, 1971, pp. 351–400.

[37] R. J. LeVeque and Z. Li. “The immersed interface method for elliptic equations with discontinuous coefficients and singular sources”. In: *SIAM Journal on Numerical Analysis* 31.4 (1994), pp. 1019–1044.

[38] Z. Li. “The immersed interface method using a finite element formulation”. In: *Applied Numerical Mathematics* 27.3 (1998), pp. 253–267.

[39] Z. Li, T. Lin, and X. Wu. “New Cartesian grid methods for interface problems using the finite element formulation”. In: *Numerische Mathematik* 96 (2003), pp. 61–98.

[40] R. J. MacKinnon and G. F. Carey. “Treatment of material discontinuities in finite element computations”. In: *International Journal for Numerical Methods in Engineering* 24.2 (1987), pp. 393–417.

[41] U. M. Mayer, A. Gerstenberger, and W. A. Wall. "Interface handling for three-dimensional higher-order XFEM-computations in fluid–structure interaction". In: *International Journal for Numerical Methods in Engineering* 79.7 (2009), pp. 846–869.

[42] N. Moës, J. Dolbow, and T. Belytschko. "A finite element method for crack growth without remeshing". In: *International Journal for Numerical Methods in Engineering* 46.1 (1999), pp. 131–150.

[43] R. A. Nicolaides. "Existence, Uniqueness and Approximation for Generalized Saddle Point Problems". en. In: *SIAM Journal on Numerical Analysis* 19.2 (1982), pp. 349–357.

[44] C. S. Peskin. "The immersed boundary method". In: *Acta numerica* 11 (2002), pp. 479–517.

[45] V. K. Saul'ev. "A method for automatization of the solution of boundary value problems on high performance computers". In: *Dokl. Akad. Nauk. SSSR (in Russian)* 144 (1962), pp. 497–500.

[46] T. Sawada and A. Tezuka. "LLM and X-FEM based interface modeling of fluid–thin structure interactions on a non-interface-fitted mesh". In: *Computational Mechanics* 48 (2011), pp. 319–332.

[47] A. Sharma and K. Maute. "Stress-based topology optimization using spatial gradient stabilized XFEM". In: *Structural and Multidisciplinary Optimization* 57 (2018), pp. 17–38.

[48] C. Wang and P. Sun. "A Fictitious Domain Method with Distributed Lagrange Multiplier for Parabolic Problems With Moving Interfaces". en. In: *Journal of Scientific Computing* 70.2 (2017), pp. 686–716.

[49] Z. Yu. "A DLM/FD method for fluid/flexible-body interactions". In: *Journal of computational physics* 207.1 (2005), pp. 1–27.

[50] A. Ženíšek. "The finite element method for nonlinear elliptic equations with discontinuous coefficients". In: *Numerische Mathematik* 58 (1990), pp. 51–77.

[51] S. Zonca, C. Vergara, and L. Formaggia. "An unfitted formulation for the interaction of an incompressible fluid with a thick structure via an XFEM/DG approach". In: *SIAM Journal on Scientific Computing* 40.1 (2018), B59–B84.

MOX Technical Reports, last issues

Dipartimento di Matematica
Politecnico di Milano, Via Bonardi 9 - 20133 Milano (Italy)

56/2023 Regazzoni, F.
An optimally convergent Fictitious Domain method for interface problems

55/2023 Orlando, G; Barbante, P.F.; Bonaventura, L.
On the evolution equations of interfacial variables in two-phase flows

54/2023 Orlando, G.
An implicit DG solver for incompressible two-phase flows with an artificial compressibility formulation

53/2023 Rossi, A.; Cappozzo, A.; Ieva, F.
Functional Boxplot Inflation Factor adjustment through Robust Covariance Estimators

52/2023 Antonietti, P.F.; Botti, M.; Mazzieri, I.
A space-time discontinuous Galerkin method for coupled poroelasticity-elasticity problems

51/2023 Bucelli, M.; Regazzoni, F.; Dede', L.; Quarteroni, A.
Preserving the positivity of the deformation gradient determinant in intergrid interpolation by combining RBFs and SVD: application to cardiac electromechanics

49/2023 Ieva, F.; Ronzulli, M.; Romo, J.; Paganoni, A.M.
A Spearman Dependence Matrix for Multivariate Functional Data

48/2023 Renzi, F.; Vergara, C.; Fedele, M.; Giambruno, V.; Quarteroni, A.; Puppini, G.; Luciani, G.B.
Accurate and Efficient 3D Reconstruction of Right Heart Shape and Motion from Multi-Series Cine-MRI

44/2023 Fontana, N.; Savaré, L.; Rea, F.; Di Angelantonio, E.; Ieva, F.
Long-term adherence to polytherapy in heart failure patients: a novel approach emphasising the importance of secondary prevention

45/2023 Gironi, P.; Petraro, L.; Santoni, S.; Dede', L.; Colosimo, B.M.
A Computational Model of Cell Viability and Proliferation of Extrusion-based 3D Bioprinted Constructs During Tissue Maturation Process